Astronomical Observing Techniques 2019

Lecture 7: Fringes, Damned Fringes and Interferometry

Huub Rottgering rottgering@strw.leidenuniv.nl

Content

- 1. Introduction
- 2. Young's slit experiment
- 3. Van Cittert Zernike relation
 - UV plane, sampling, tapering, deconvolution, self calibration
- Optical interferometers
- Radio interferometers

Very Large Array VLA

- Y-shaped array, 27 telescopes on railroad tracks
- 25-m diameter telescopes, New Mexico, USA
- Configurations spanning 1.0, 3.4, 11, and 36 km



Cygnus A at 6 cm with VLA

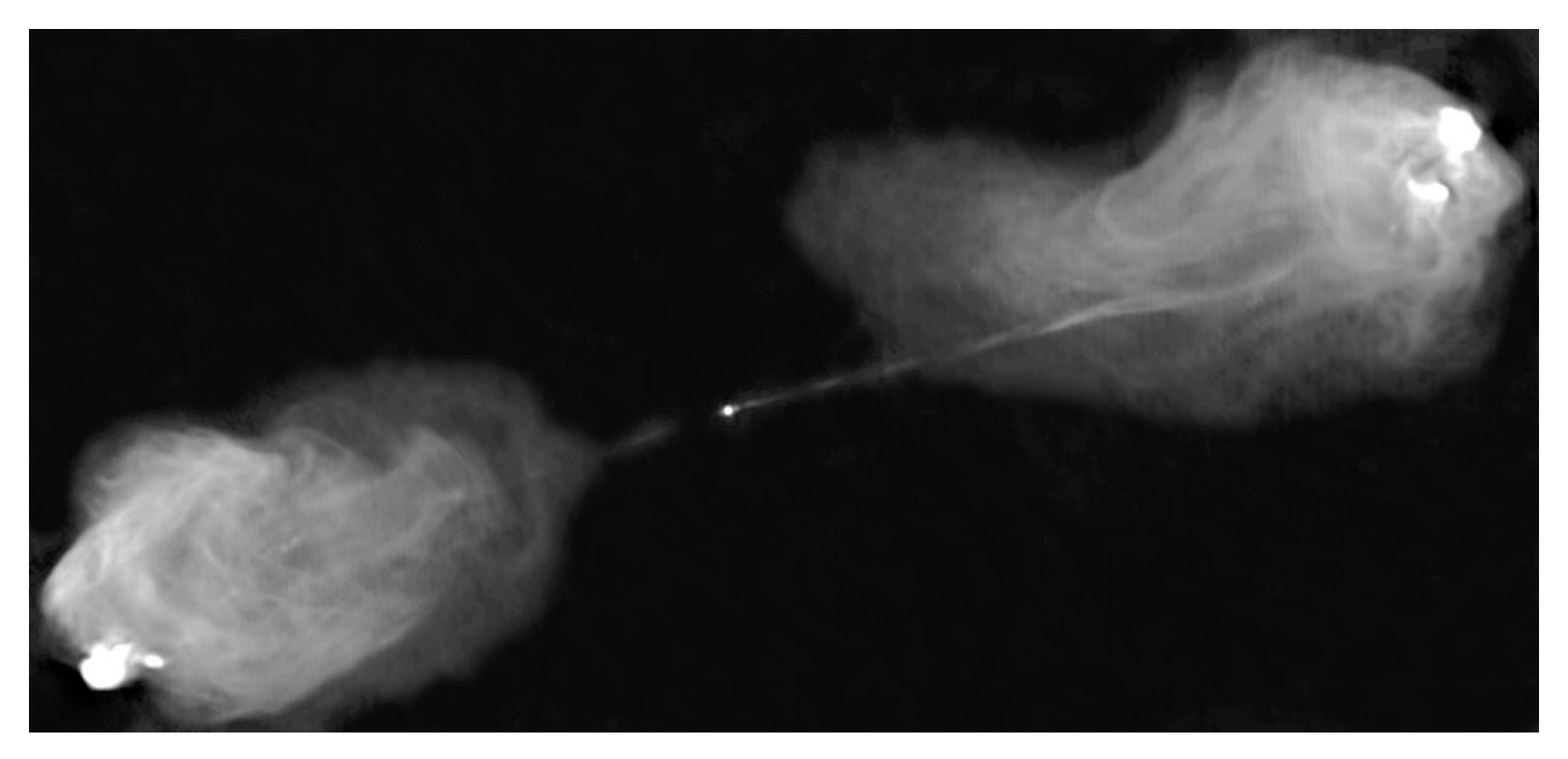
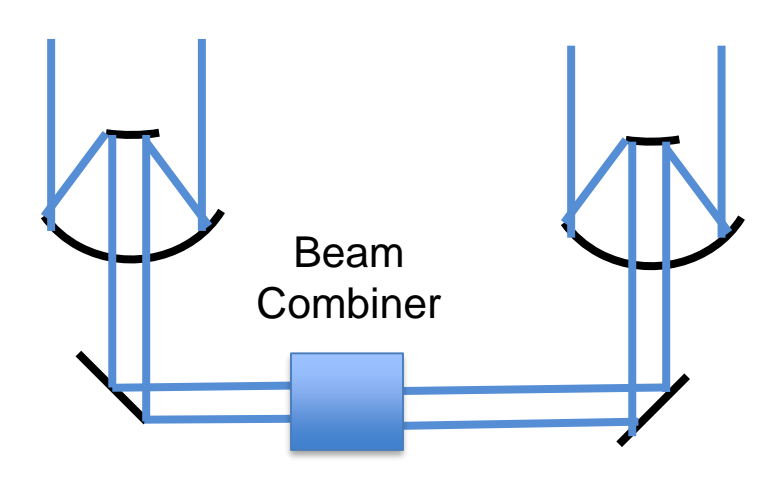


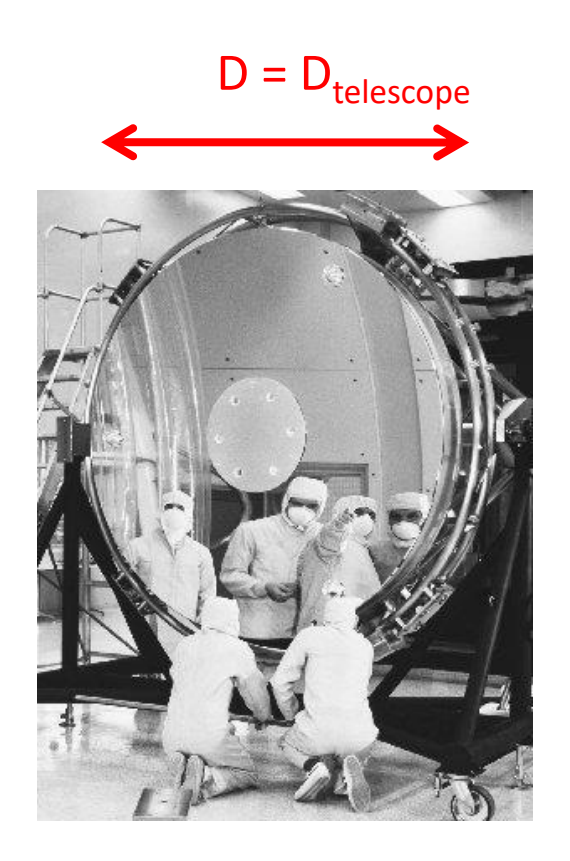
Image courtesy of NRAO/AUI

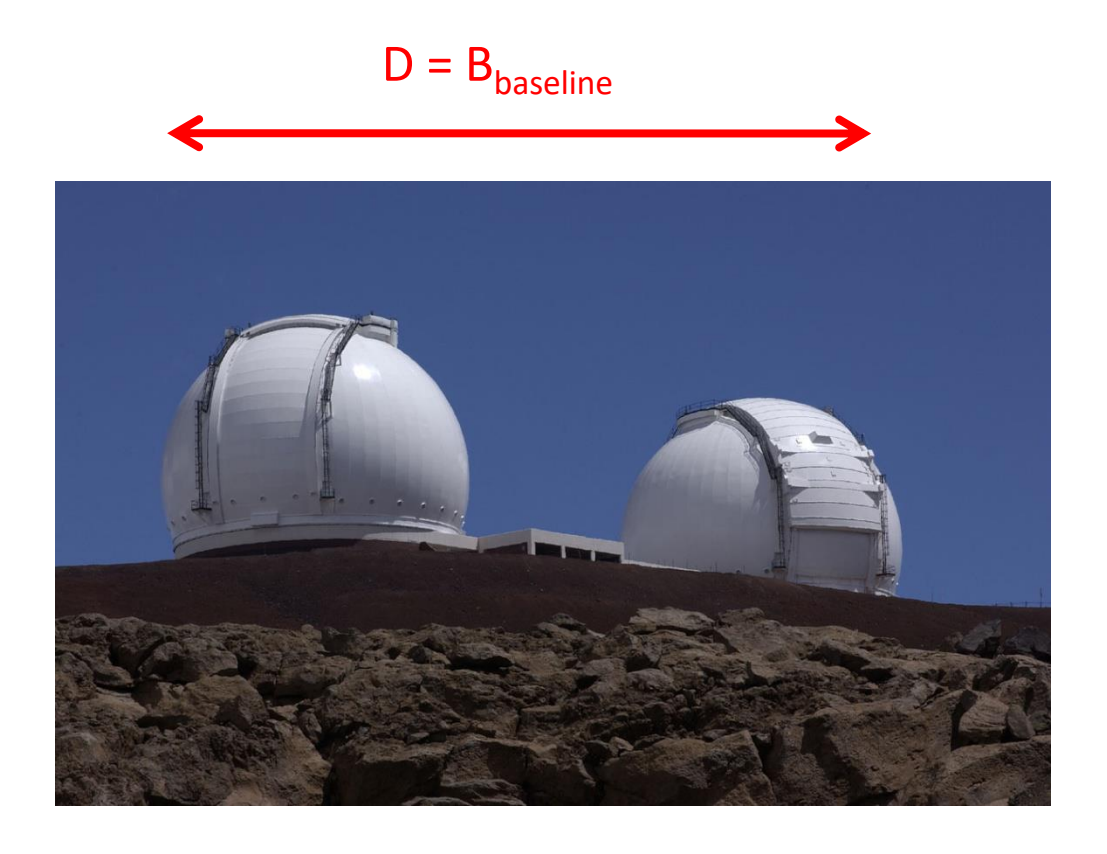
Interferometers

- Goal: increase resolution
- General principle: Coherently combine ≥2 beams
- Requires accuracies of optics $\ll \lambda$



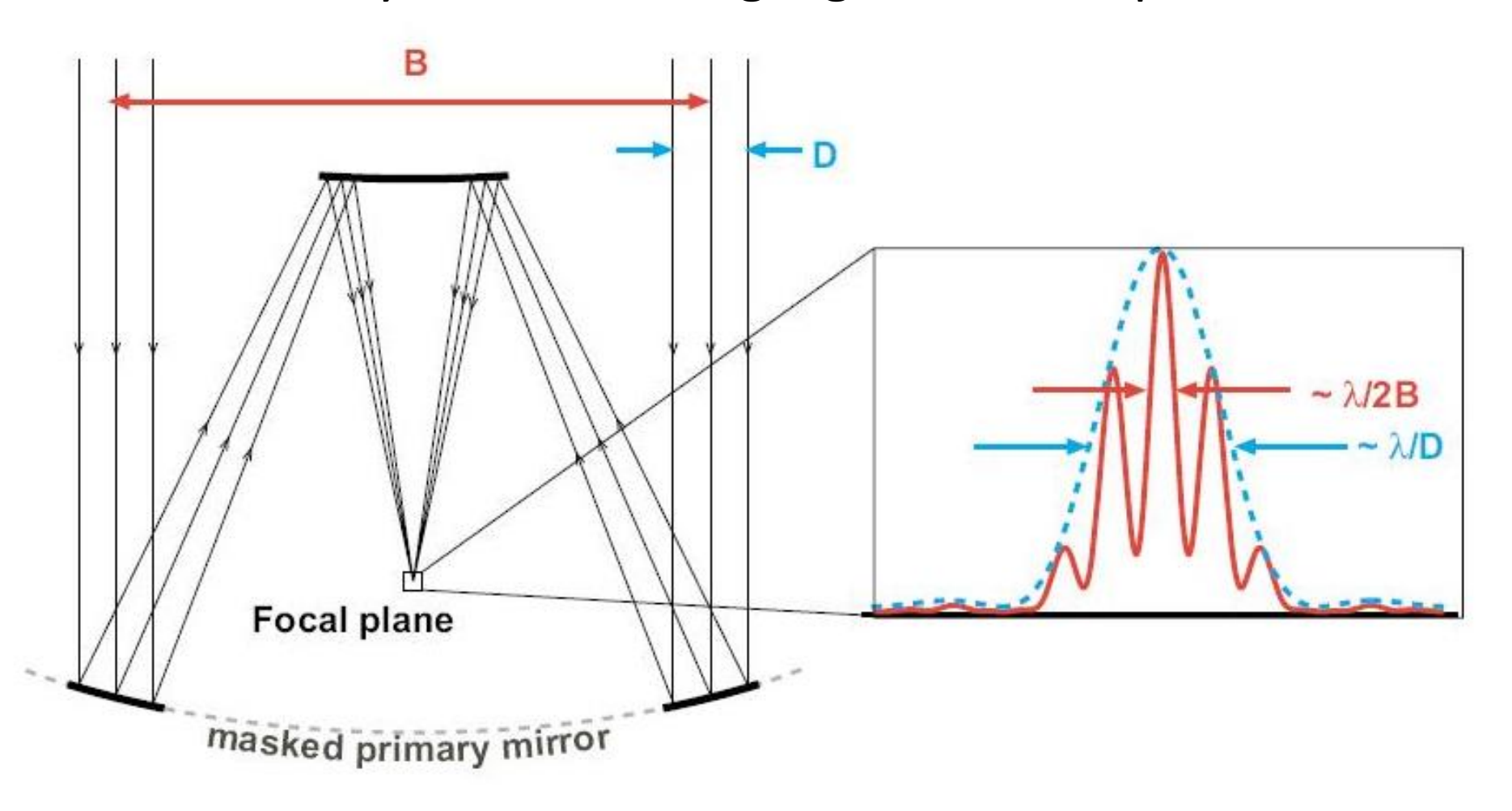
Increase Angular Resolution λ/D



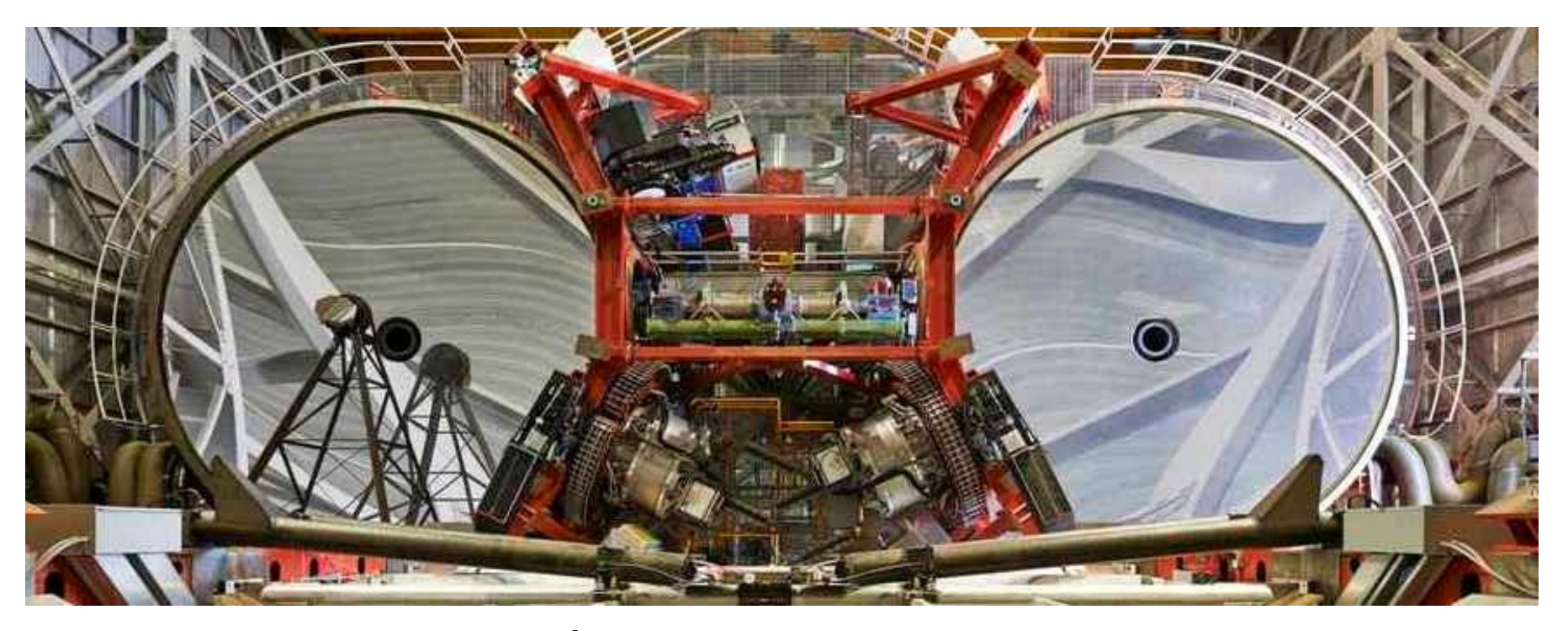


PSF of Masked Aperture

Interferometry is like masking a giant telescope:

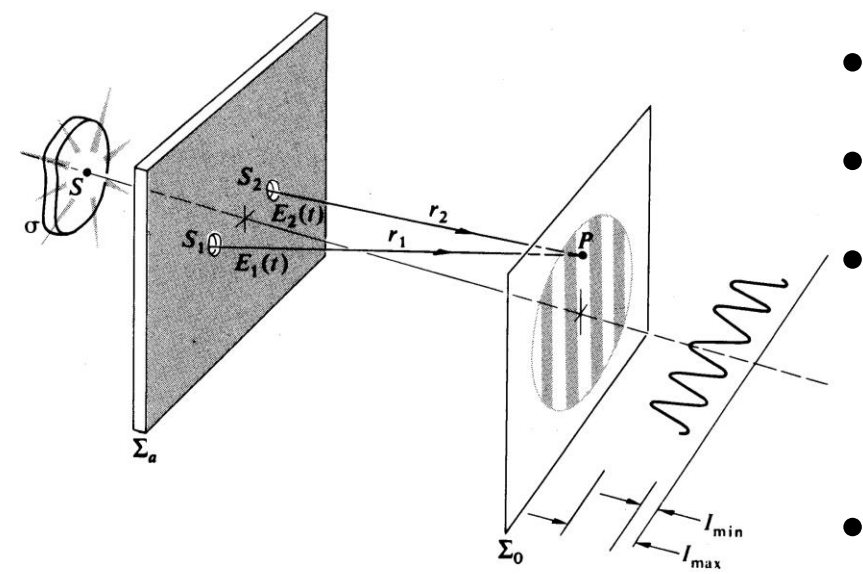


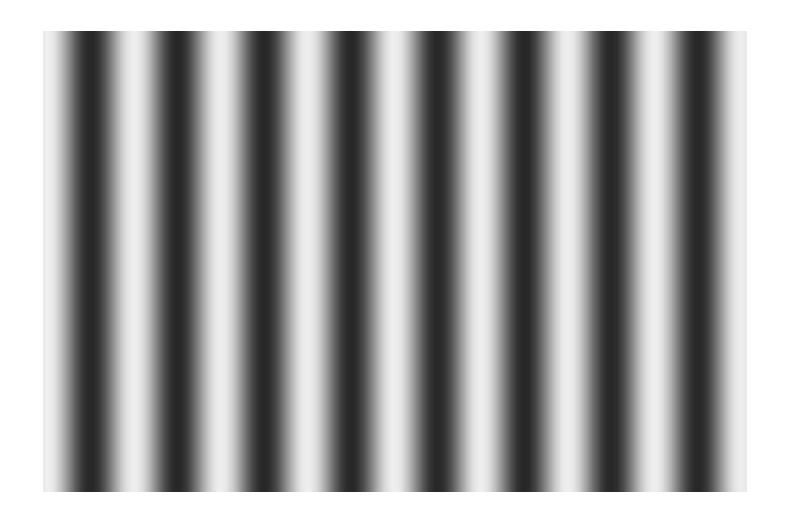
Large Binocular Telescope Interferometer



- Two 8.4-meter telescopes on common mount
- 23 m from edge to edge
- Beam-combiner is green/silver unit between telescopes

Young's Double Slit Experiment





- monochromatic wave
- infinitely small pinholes
- source S generates fields

$$- E(r_1,t) = E_1(t) \text{ at } S_1$$

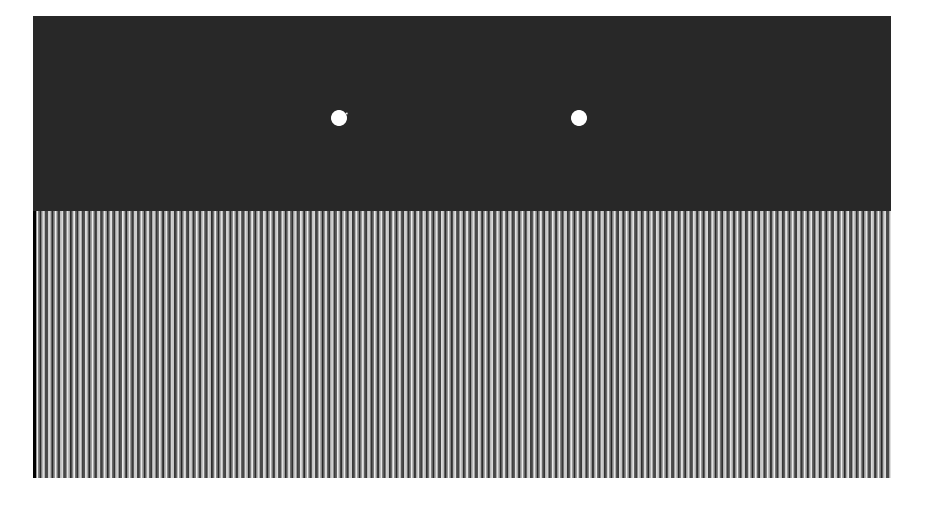
$$- E(r_2,t) = E_2(t)$$
 at S_2

- two spherical waves from pinholes interfere on screen
- electrical field at P is sum of electrical field originating from S₁ and S₂
- Maxima if path lengths differences are k*wavelength

Dual Pinhole Interferometer

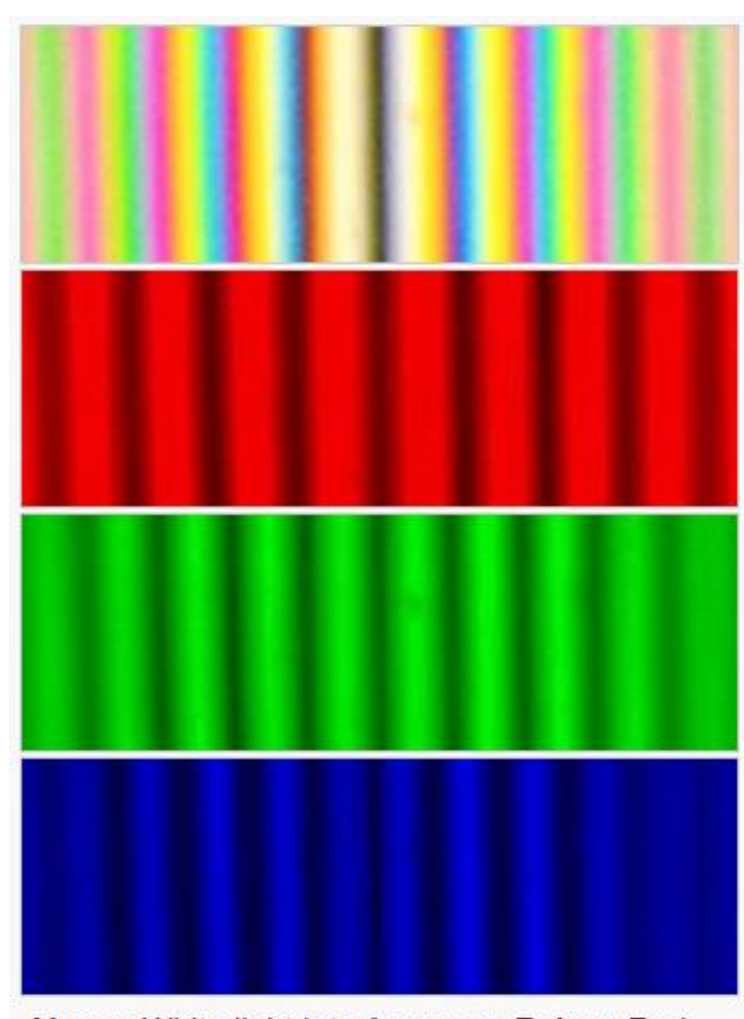
- Assume that telescope diameter D ≪ baseline B (telescope separation)
- Looking at point source at single wavelength λ
- Same as Young's double slit setup
- Fringes with a spacing $\sim \lambda/B$





Broadband Fringes

- Fringe spacing is proportional to wavelength λ
- Broadband light will smear fringes
- Central fringe (white light fringe)
 has highest contrast
- Interferometers limit wavelength range to optimize fringe contrast
- Need to work around zero pathlength difference

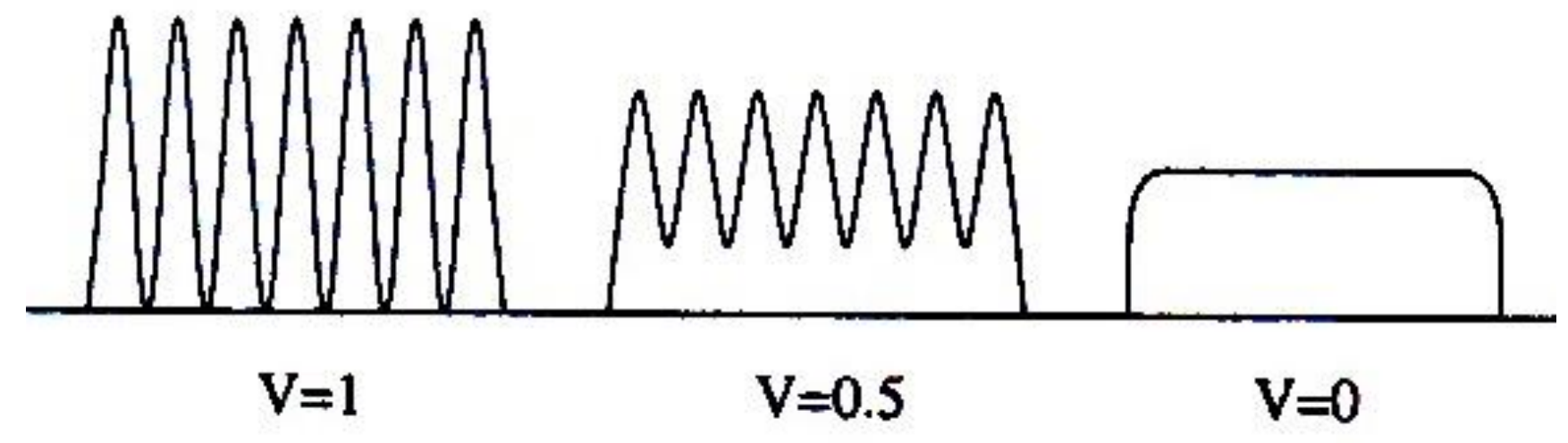


Above: White light Interferogram, Below: Red-, Green- and Blue channels of the White light interferogram shown above

Visibility

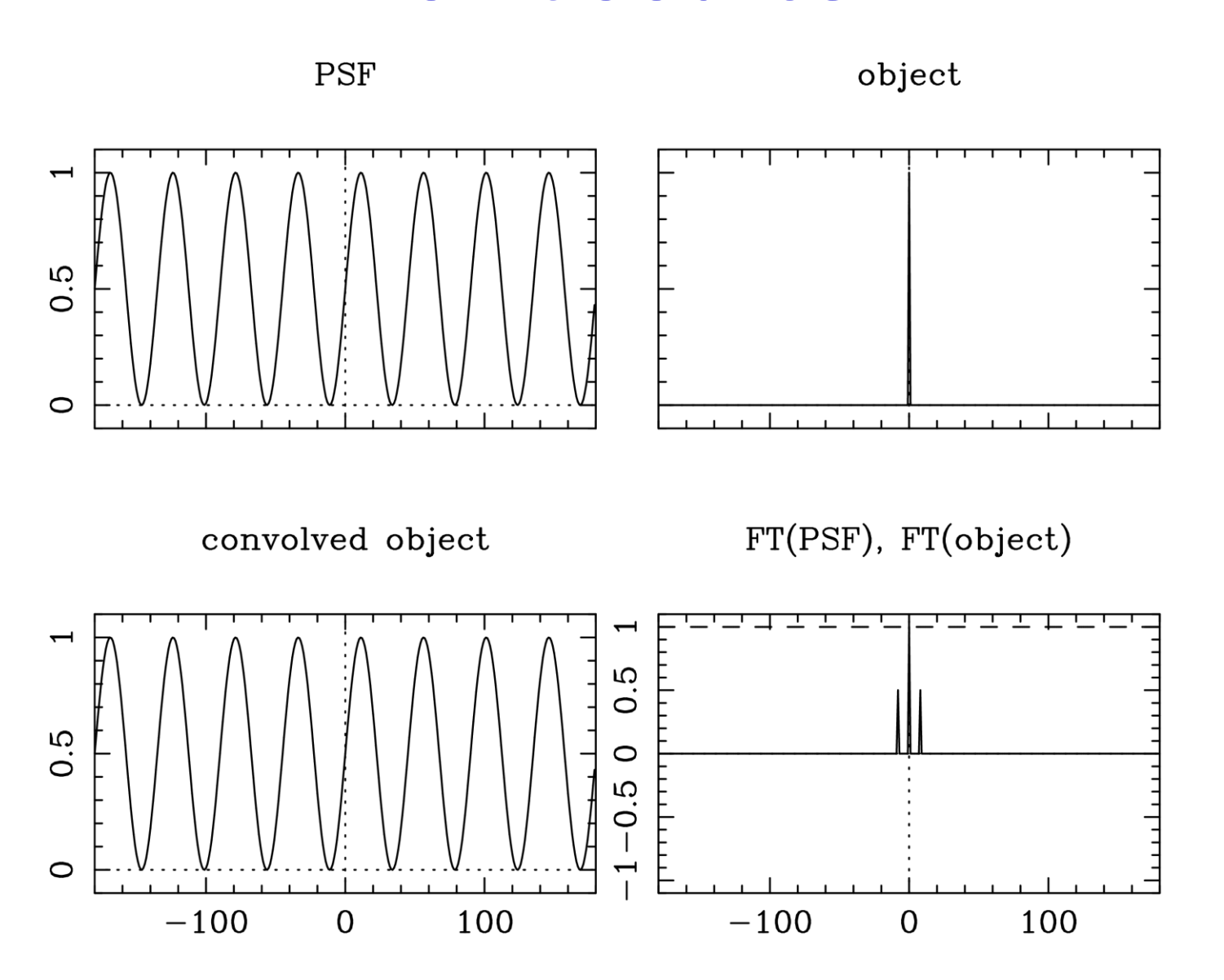
Fringe visibility

$$V = \frac{I_{\text{max}} - I_{\text{min}}}{I_{\text{max}} + I_{\text{min}}}$$

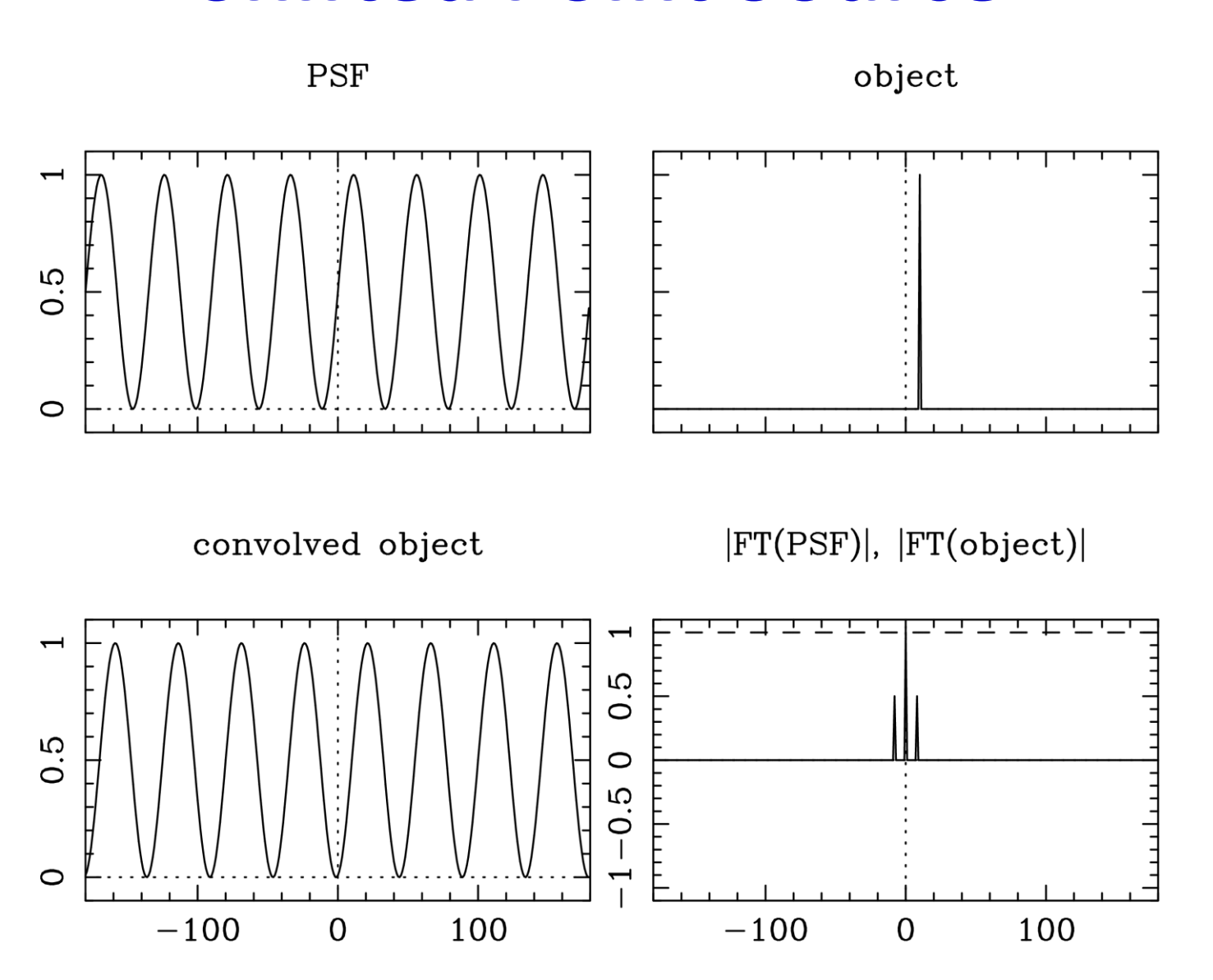


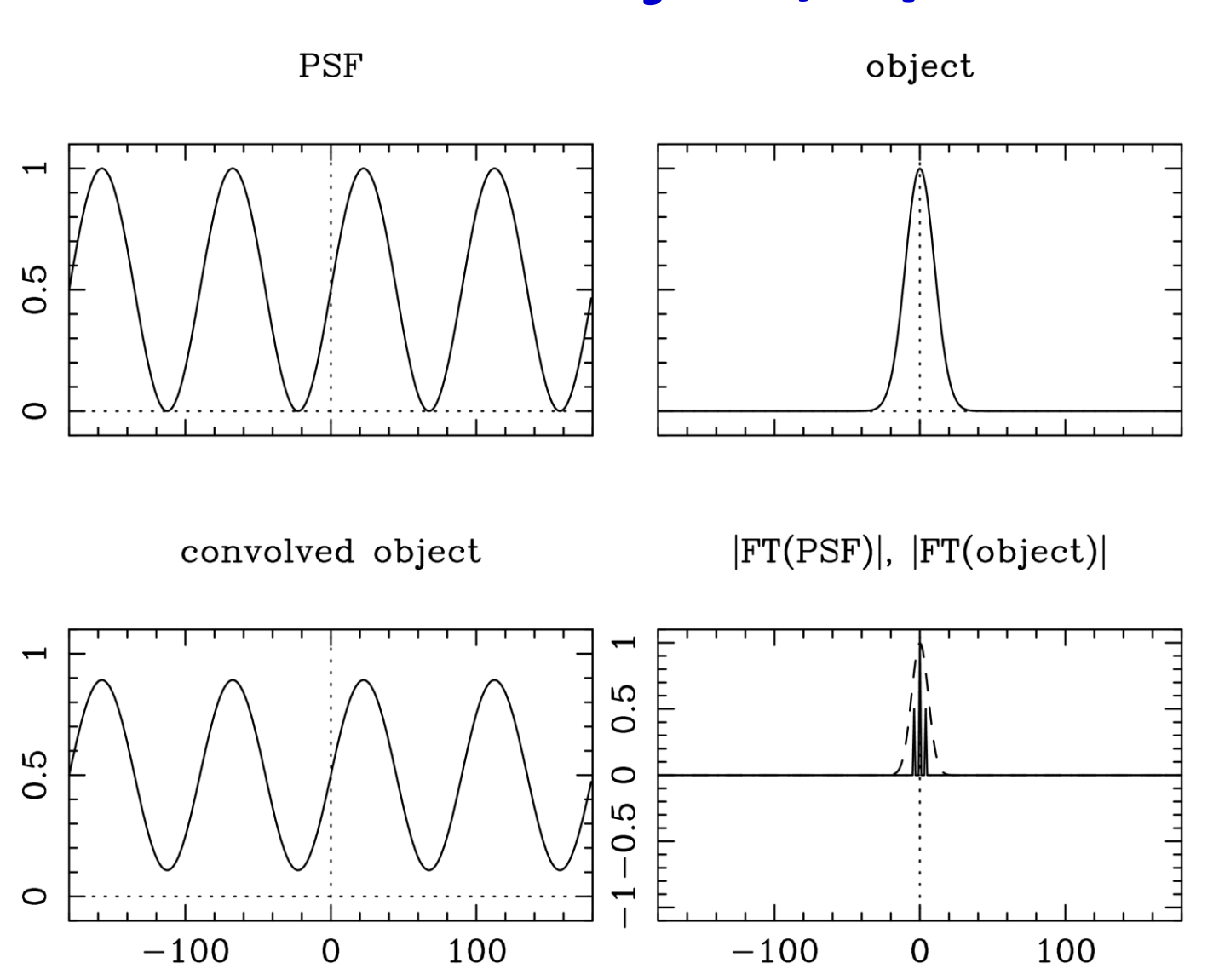
- Fringe pattern of extended object is fringe pattern of point-source (PSF) convolved with object
- Still a fringe pattern but with reduced visibility

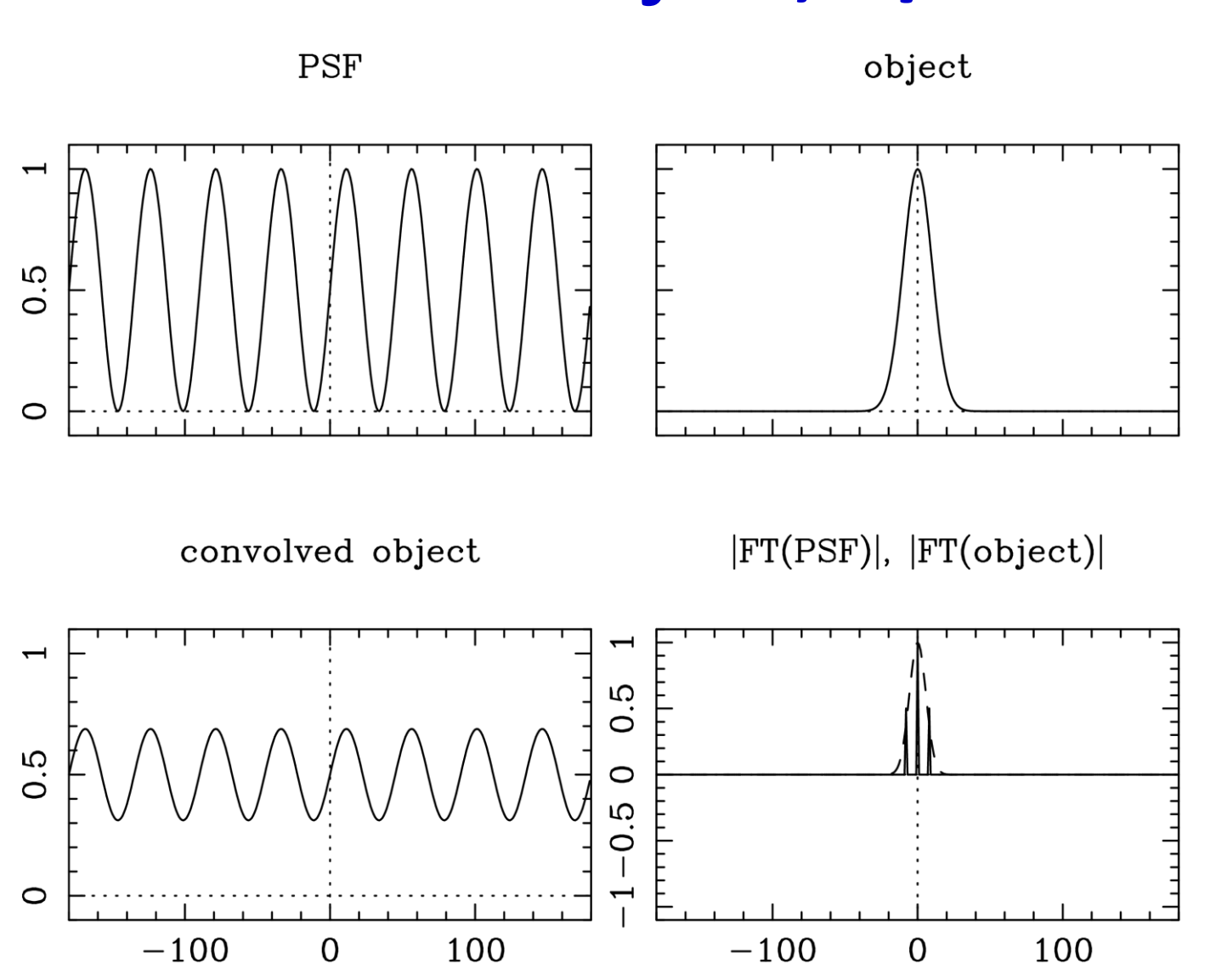
Point Source

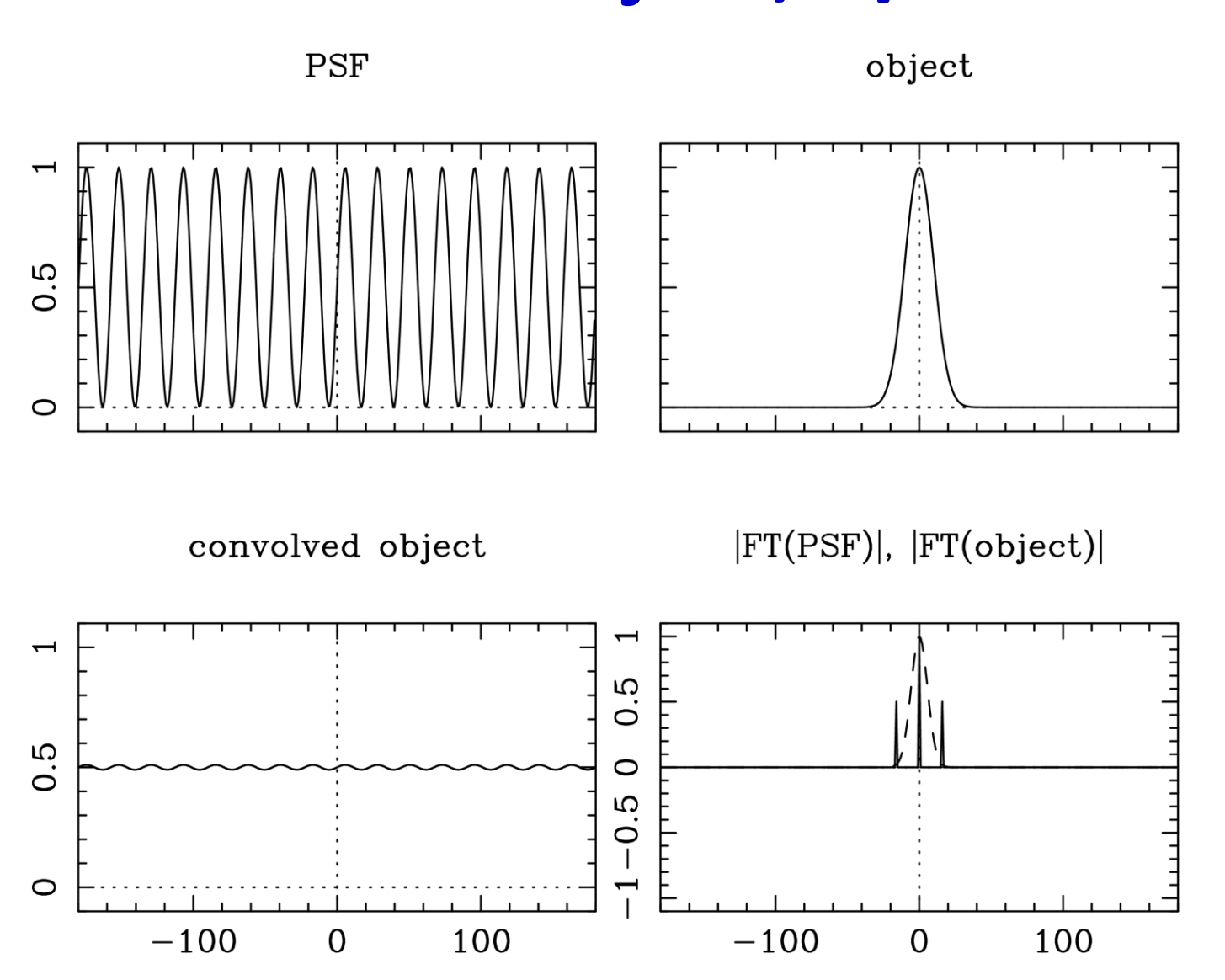


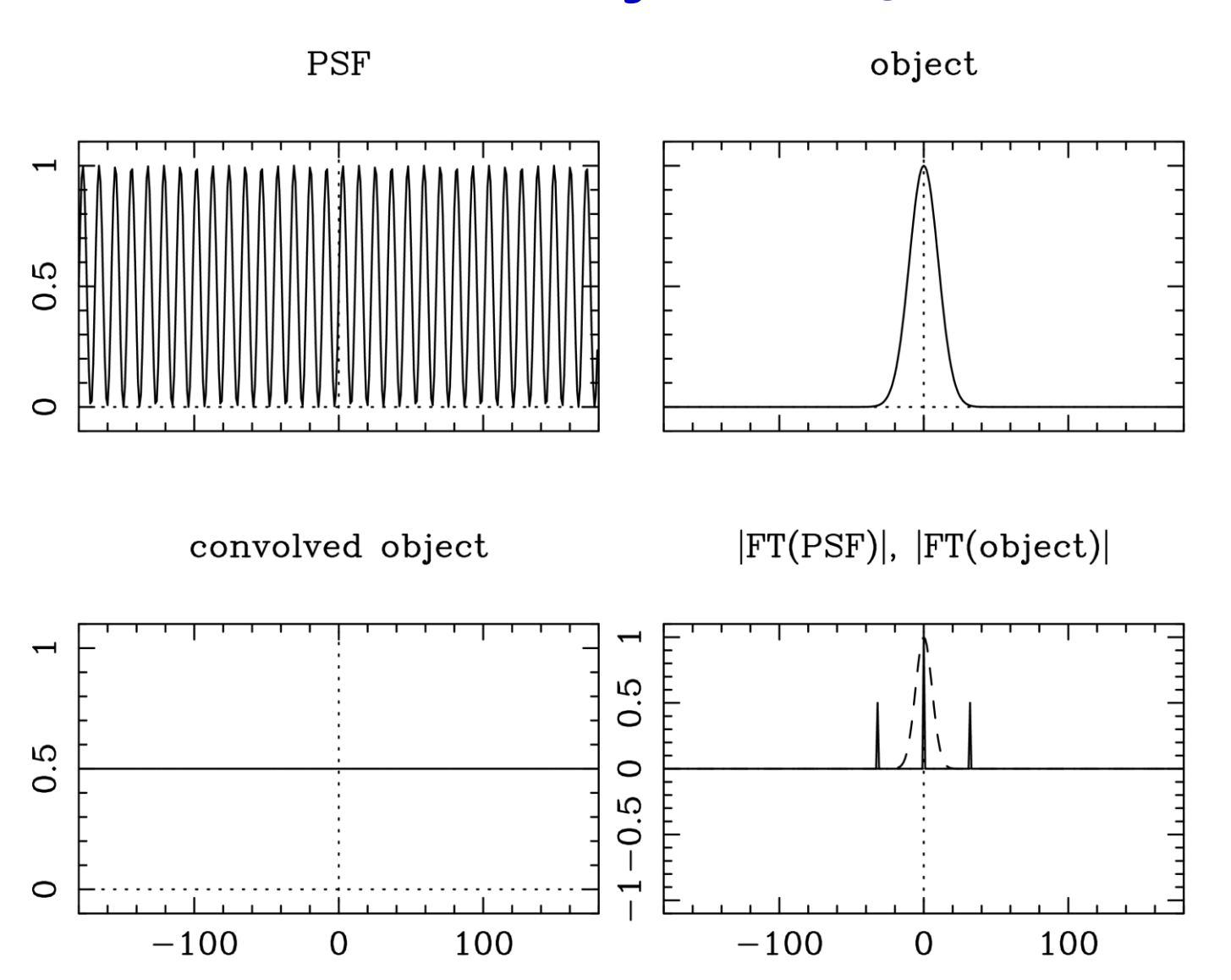
Shifted Point Source





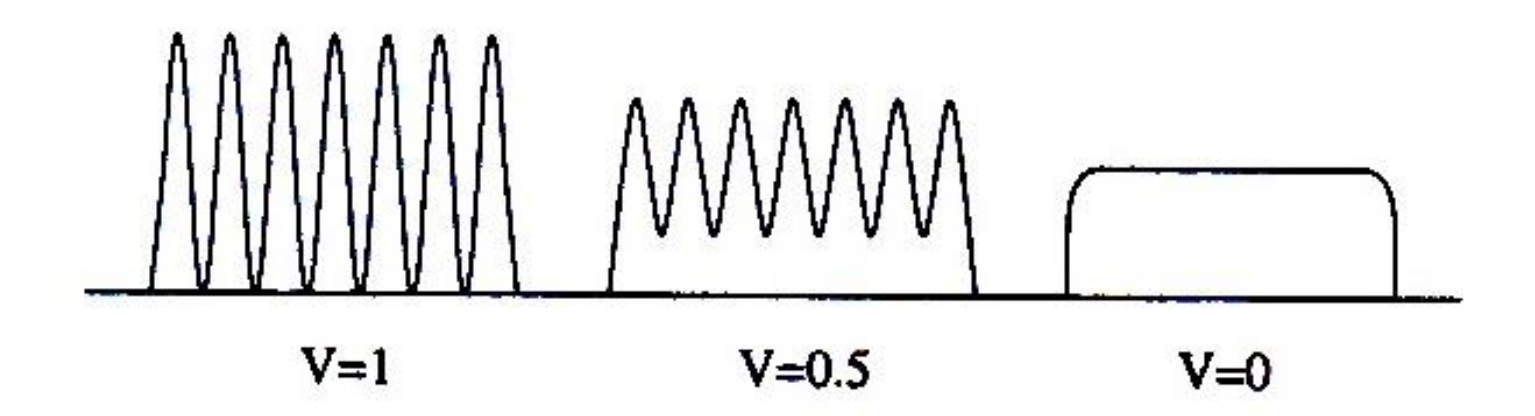






Van Cittert-Zernike Theorem

- dark regions in fringe pattern go to zero: V = 1
 → object is "unresolved"
- no fringes: V = 0 → object is completely "resolved"
- Van-Cittert Zernike theorem: Visibility is the absolute value of the Fourier transform of the object's brightness distribution



Complex visibility

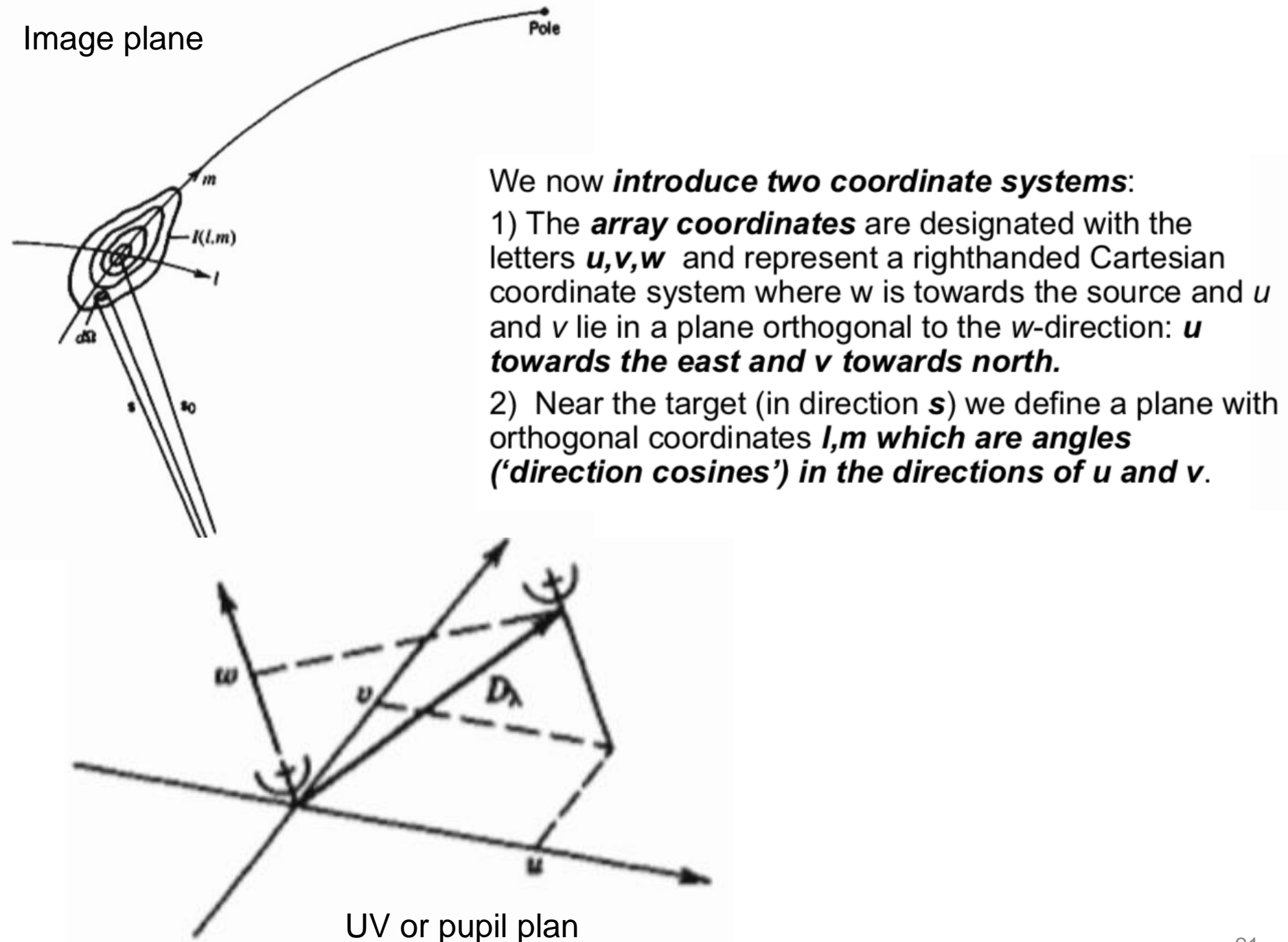
 Basic measurement is the cross-correlation of the electric field at two locations, r₁ and r₂:

$$V_{\nu}(\mathbf{r_1}, \mathbf{r_2}) = \langle E_{\nu}(\mathbf{r_1}) E_{\nu}^*(\mathbf{r_2}) \rangle$$

 Using the wavelength observed as the unit, define (u,v,w) coordinate system

$$(u, v, w) = (\mathbf{r_1} - \mathbf{r_2})/\lambda$$

• Hence the complex visibility for an interferometer in a plane: $V_{\nu}(u,v)$



The van Cittert - Zernike relation (II)

In the **small angle approximation** the visibility equation then takes on the simple 2-D form:

$$V(u,v) = \int \int I(l,m)e^{-2\pi i(ul+vm)}dldm$$

This equation is called the *van Cittert - Zernike relation* who first derived it in an optical context. The Fourier inversion of this equation leads to:

$$I(l,m) = \int \int V(u,v)e^{2\pi i(ul+vm)}dudv$$

Hence by measuring the visibility function V(u,v) we can, through a Fourier transform, derive the brightness distribution I(l,m). Therefore, the more u,v samples we measure the more complete our knowledge of the source structure.

Each point in the u-v plane samples one component of the Fourier transform of the brightness distribution. The points at **small u,v record large scale structure and vice-versa**.

4.3. Effect of discrete sampling

In practice the spatial coherence function V is not known everywhere but is sampled at particular places on the u-v plane. The sampling can be described by a sampling function S(u, v), which is zero where no data have been taken. One can then calculate a function

$$I_{\nu}^{D}(l, m) = \int \int V_{\nu}(u, v)S(u, v)e^{2\pi i(ul+vm)} du dv.$$
 (1-10)

Radio astronomers often refer to $I_{\nu}^{D}(l, m)$ as the dirty image; its relation to the desired intensity distribution $I_{\nu}(l, m)$ is (using the convolution theorem for Fourier transforms):

$$I_{\nu}^{D} = I_{\nu} * B$$
, (1-11)

where the in-line asterisk denotes convolution and

$$B(l, m) = \iint S(u, v)e^{2\pi i(ul+vm)} du dv$$
 (1-12)

is the synthesized beam or point spread function corresponding to the sampling function S(u, v). Equation 1–11 says that I^D is the true intensity distribution I convolved with the synthesized beam B.

Tapering

- Weighing the visibilities as a function of baseline length: $T(u,v)=T(\sqrt{u^2+v^2})$
- Often a Gaussian is used: Gaussian tapering.
- Tapering with a Gaussian with FWHM of w, gives a PSF with a FWHM of 1/w

(Radio) Aperture Synthesis

Limited information about source provided by 2-element interferometer can be expanded by moving the telescopes to change the baselines.

Even better: use N telescopes and combine their outputs:
N telescopes provide N(N-1)/2
baselines. Each baseline adds a new Fourier component (or fringe spacing)

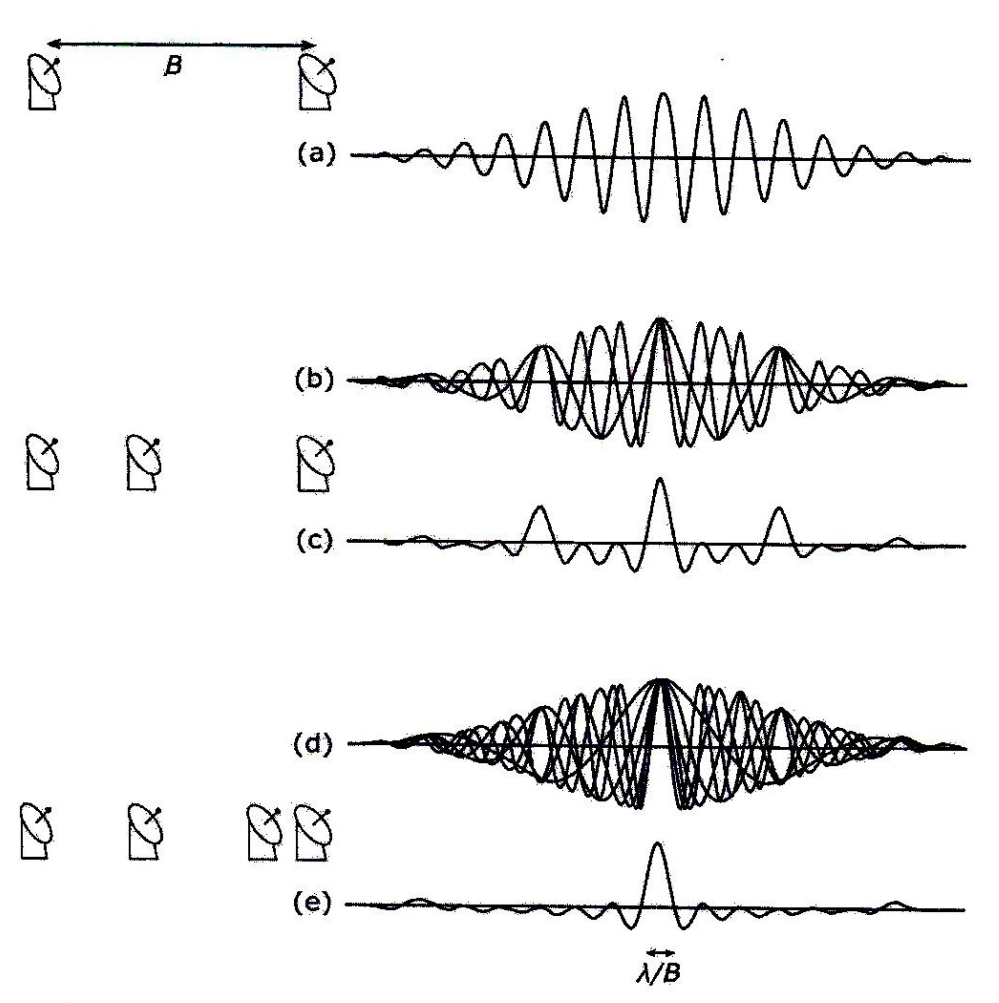
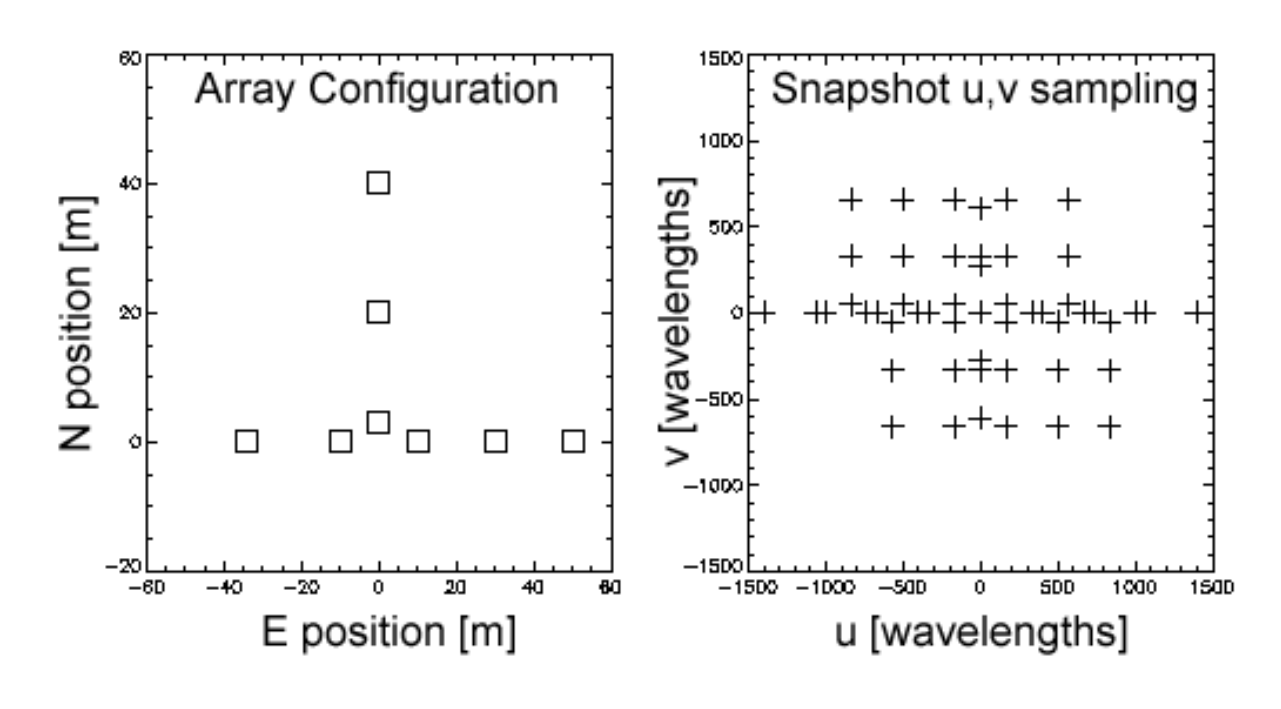
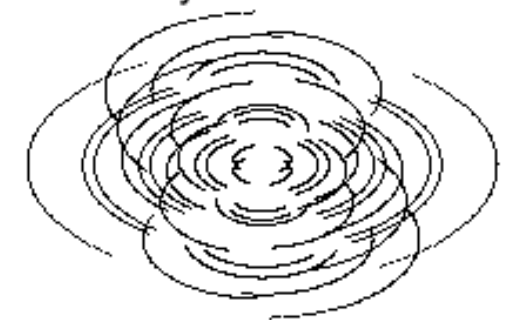


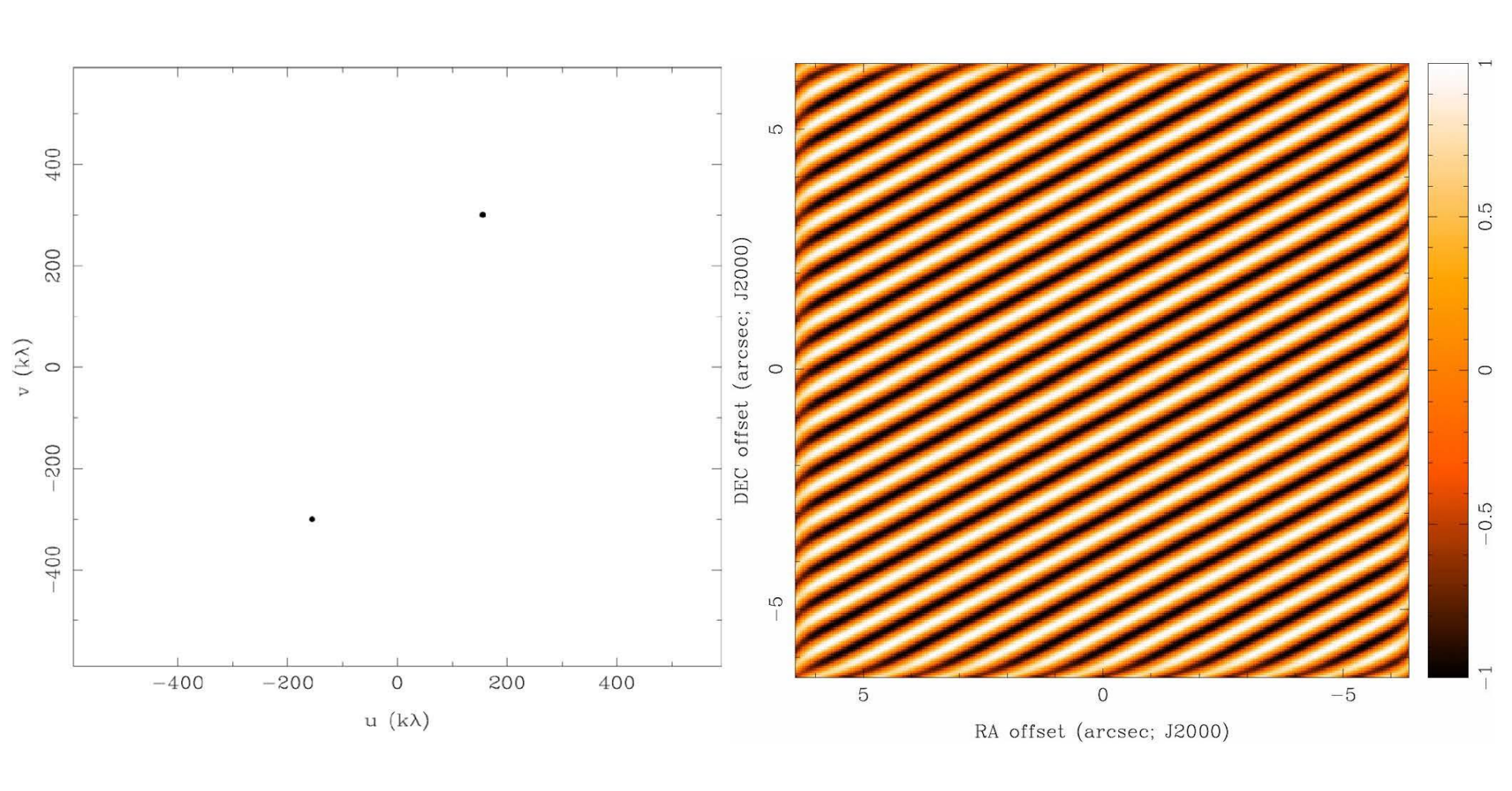
Figure 9.2. Improvement in field pattern quality (the images are the auto-correlation) with increasing number of interferometer baselines. Based on Condon and Ransom (2010).

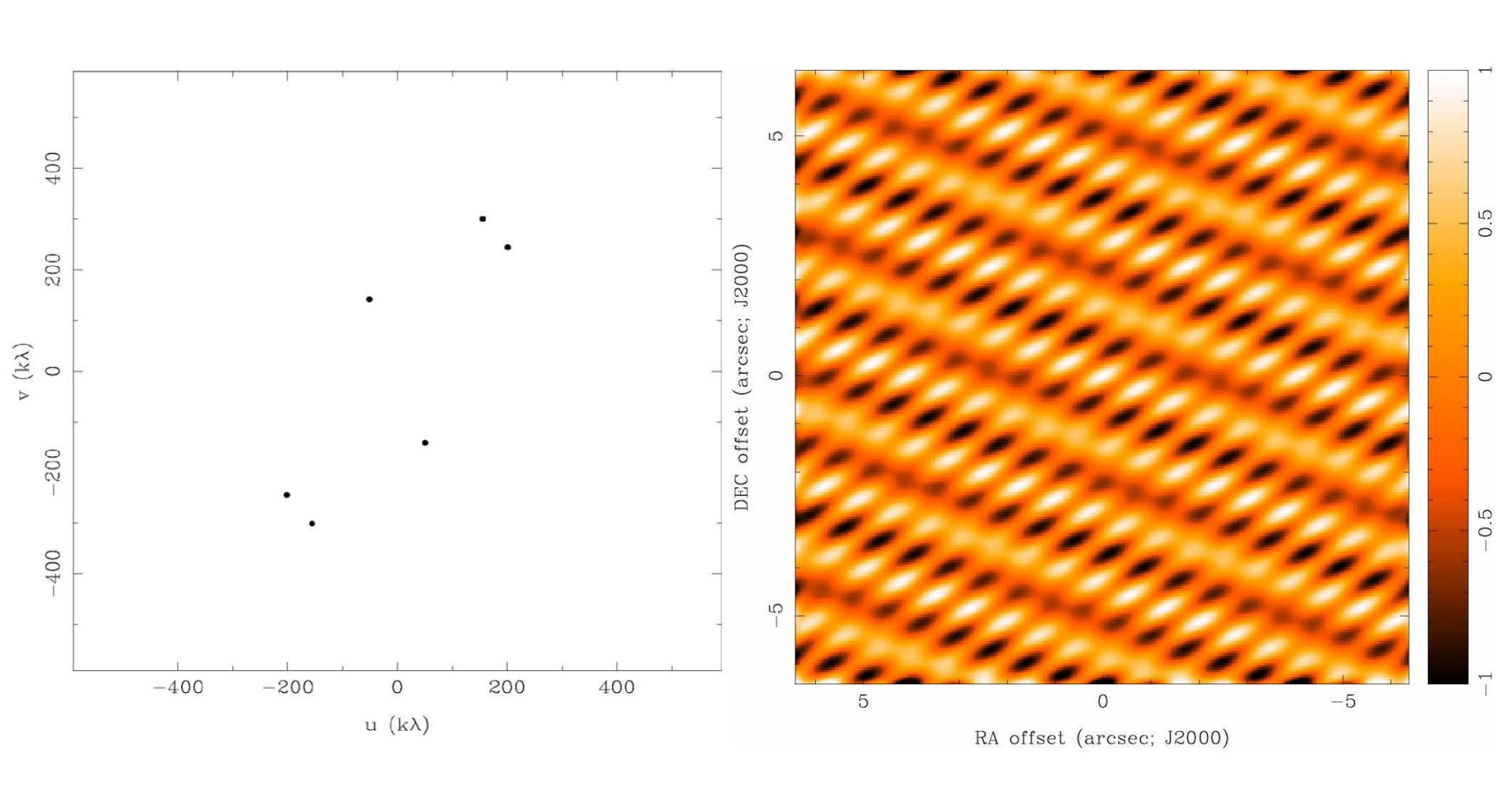


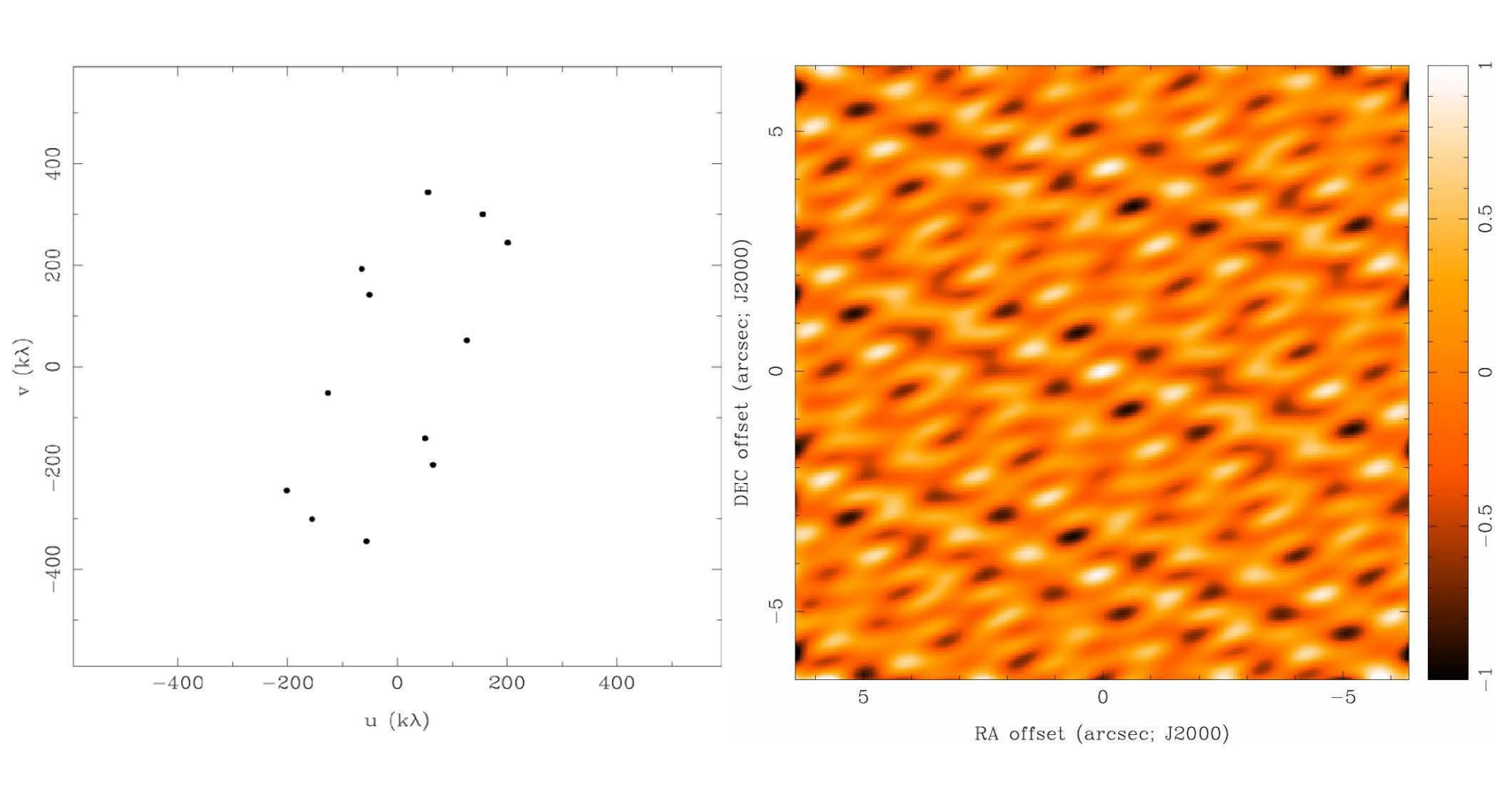
u,v sampling after 12 hour synthesis

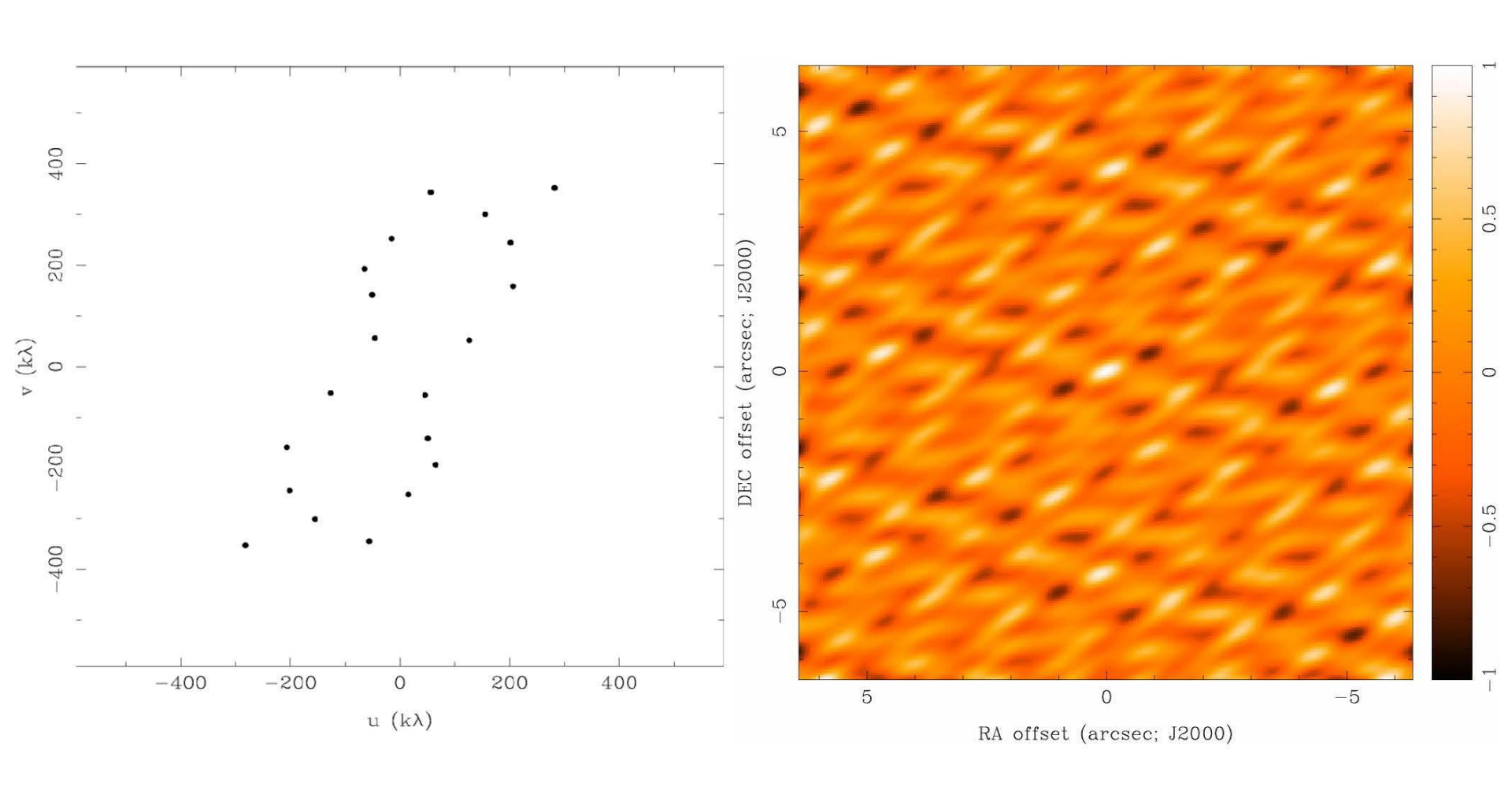


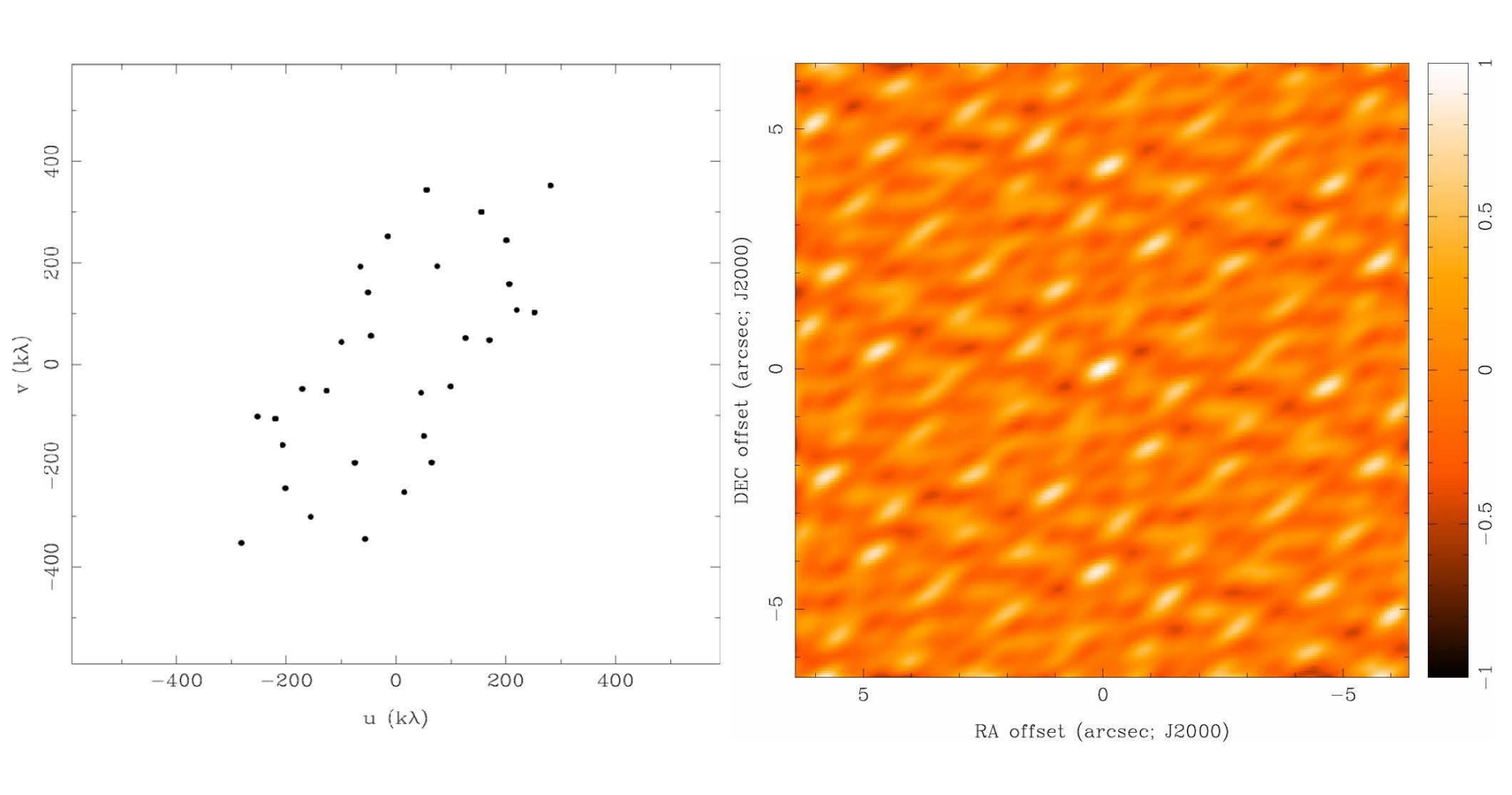
I(l,m)	(a)	B(l,m) (b)	I(l,m)*B(l,m) (c)
Map		Beam	Dirty Map
V(u,v)	(d)	S(u,v) (e)	V(u,v)S(u,v) (f)
Visibility		Sampling Function	Sampled Visibility

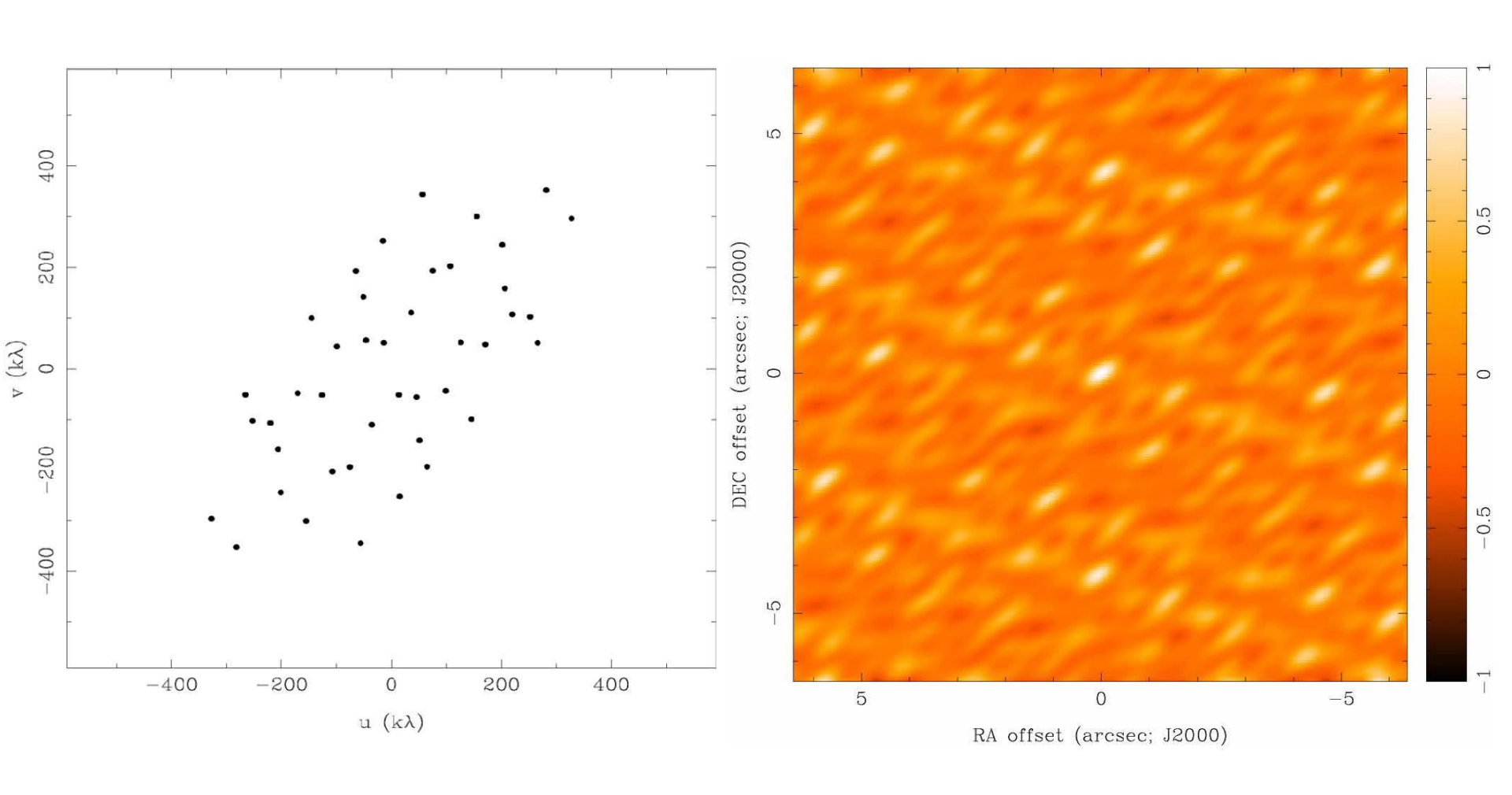


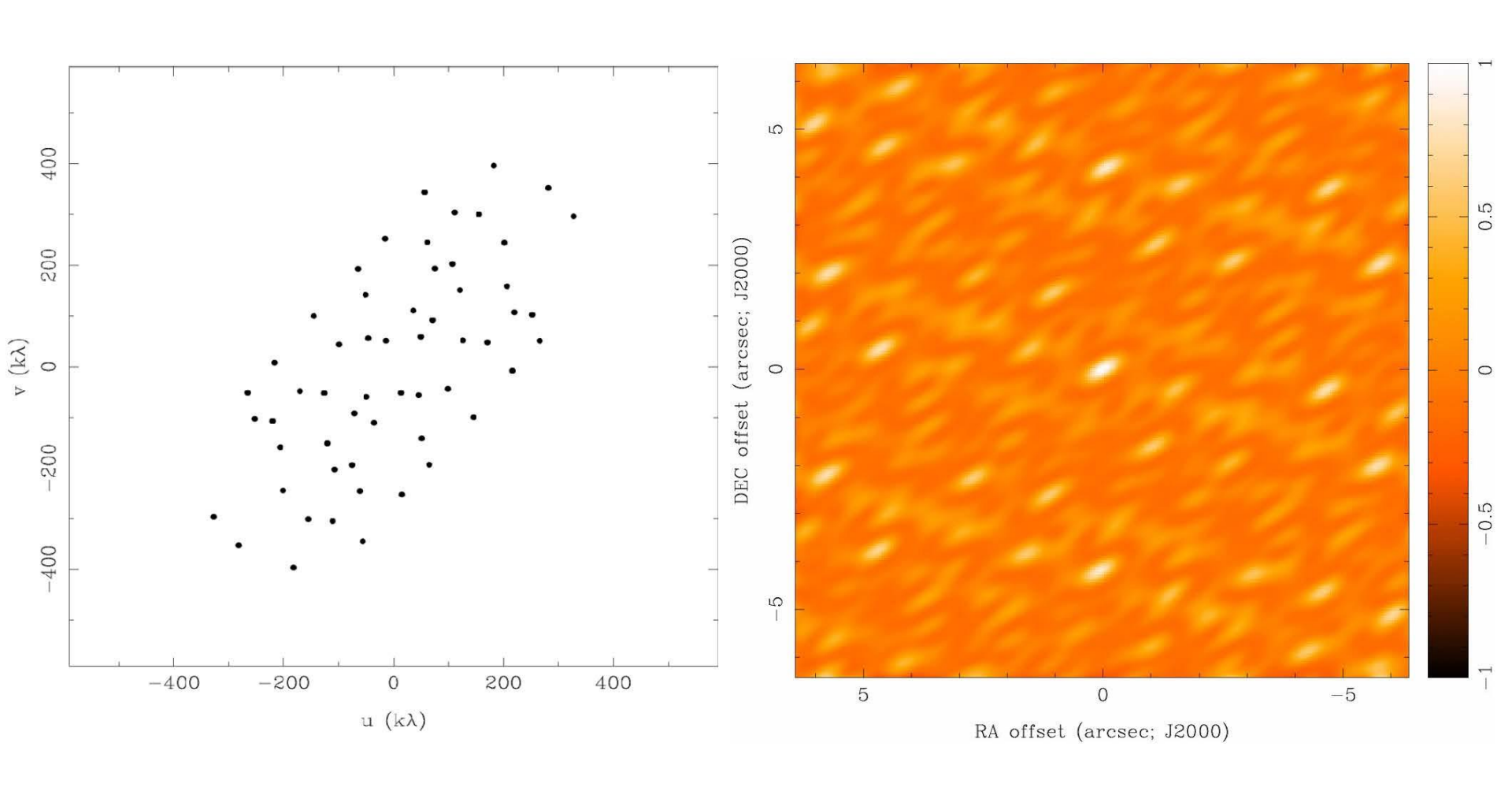




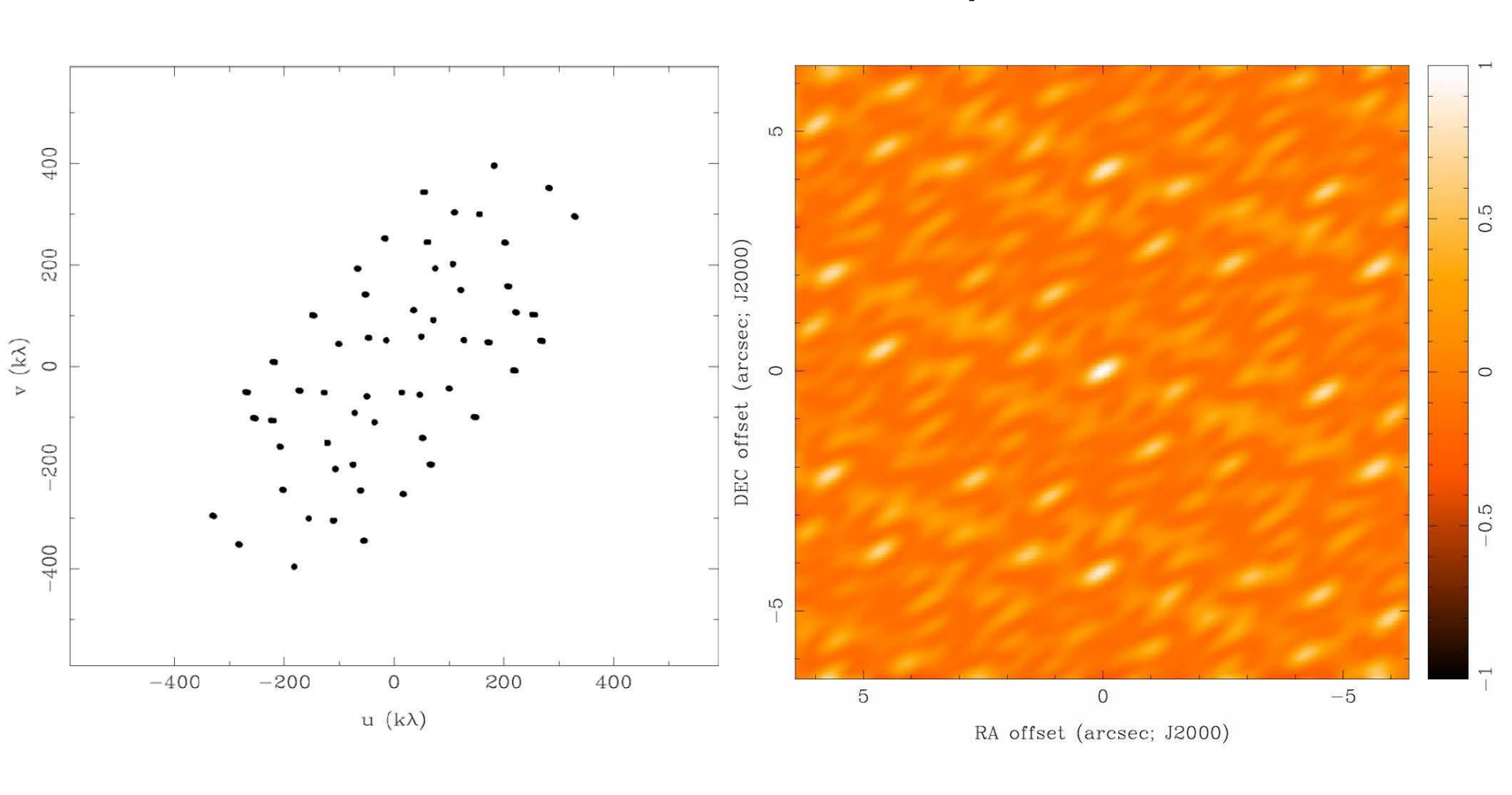




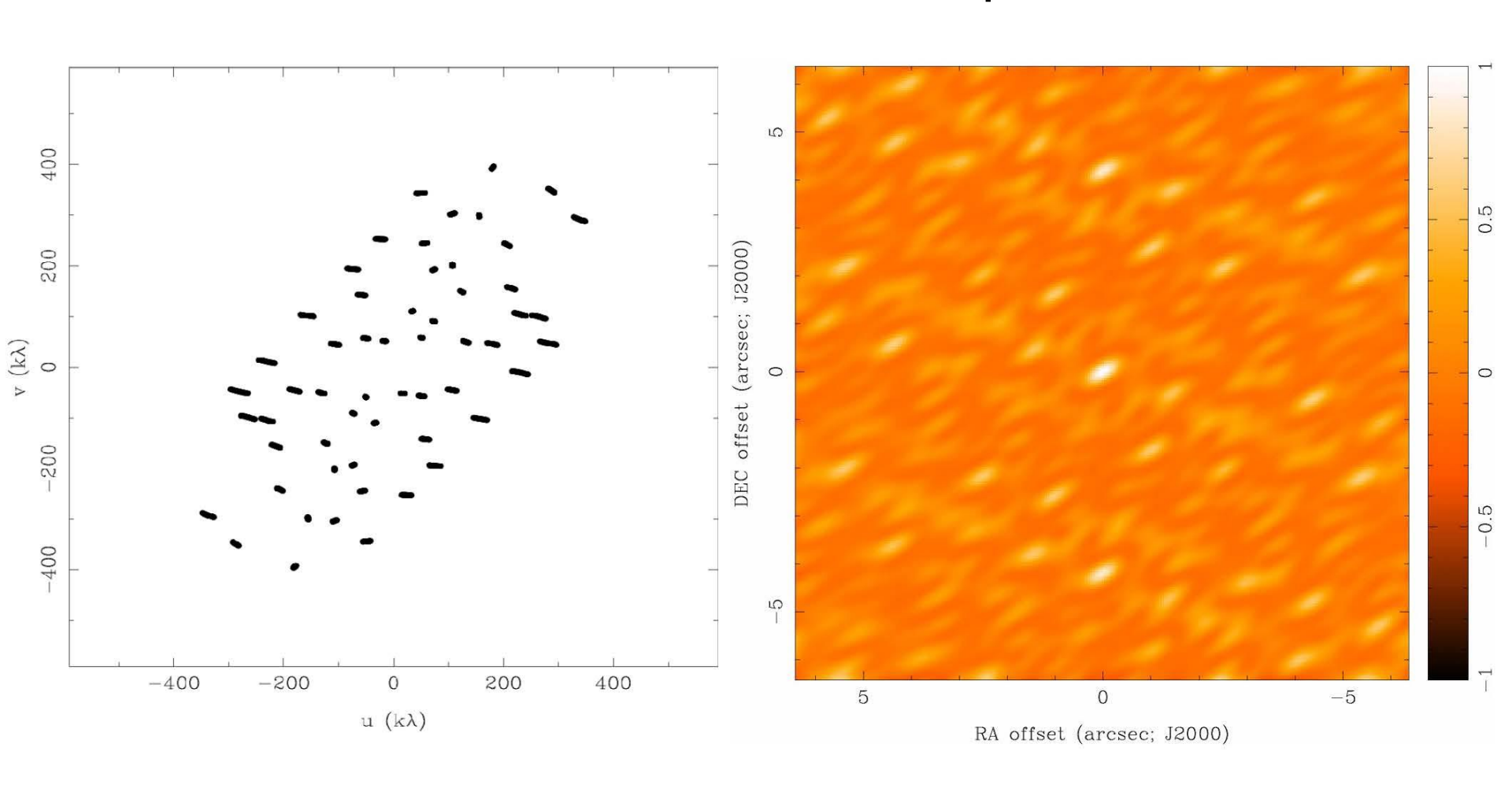




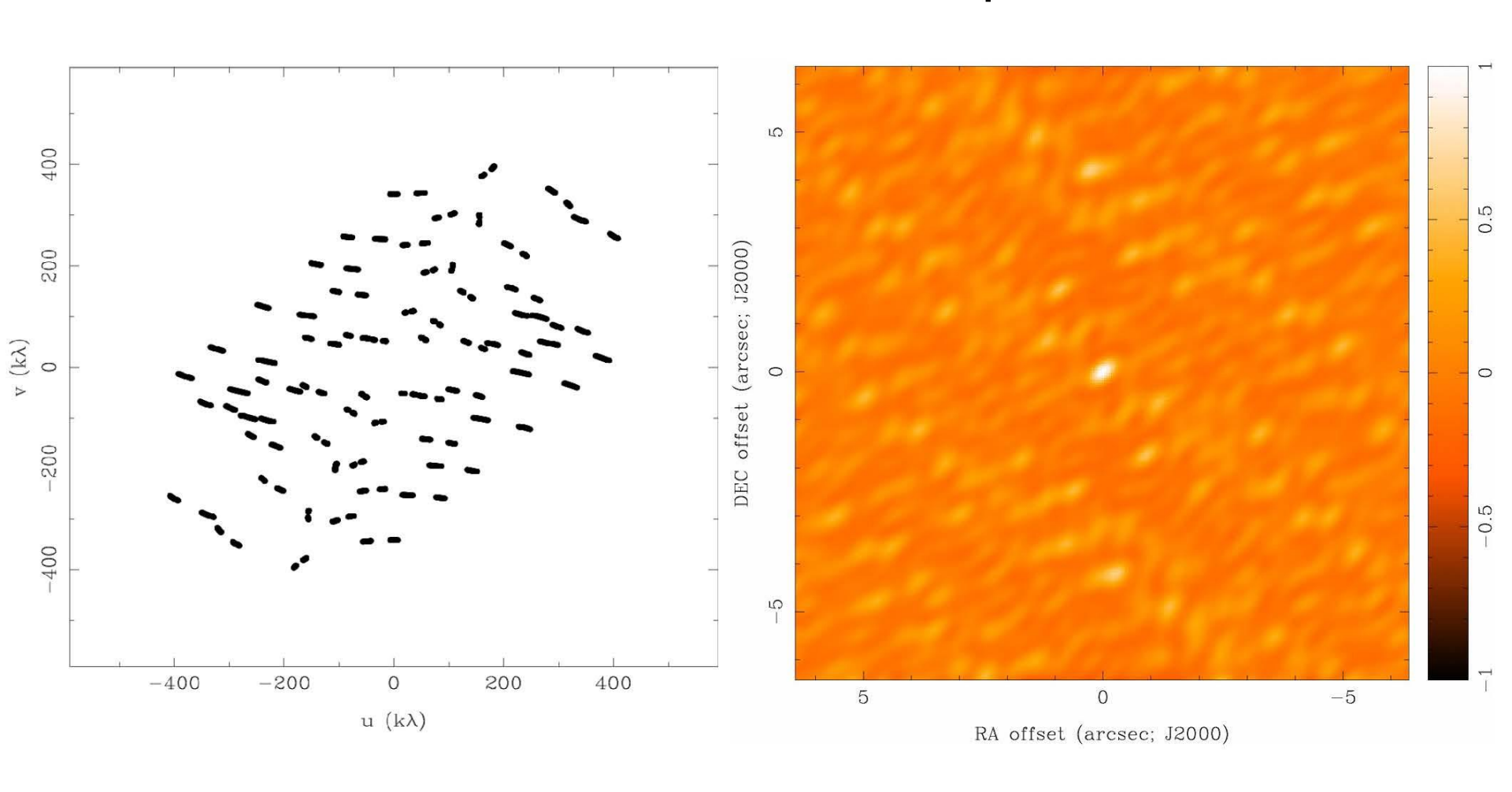
8 Antennas x 6 Samples



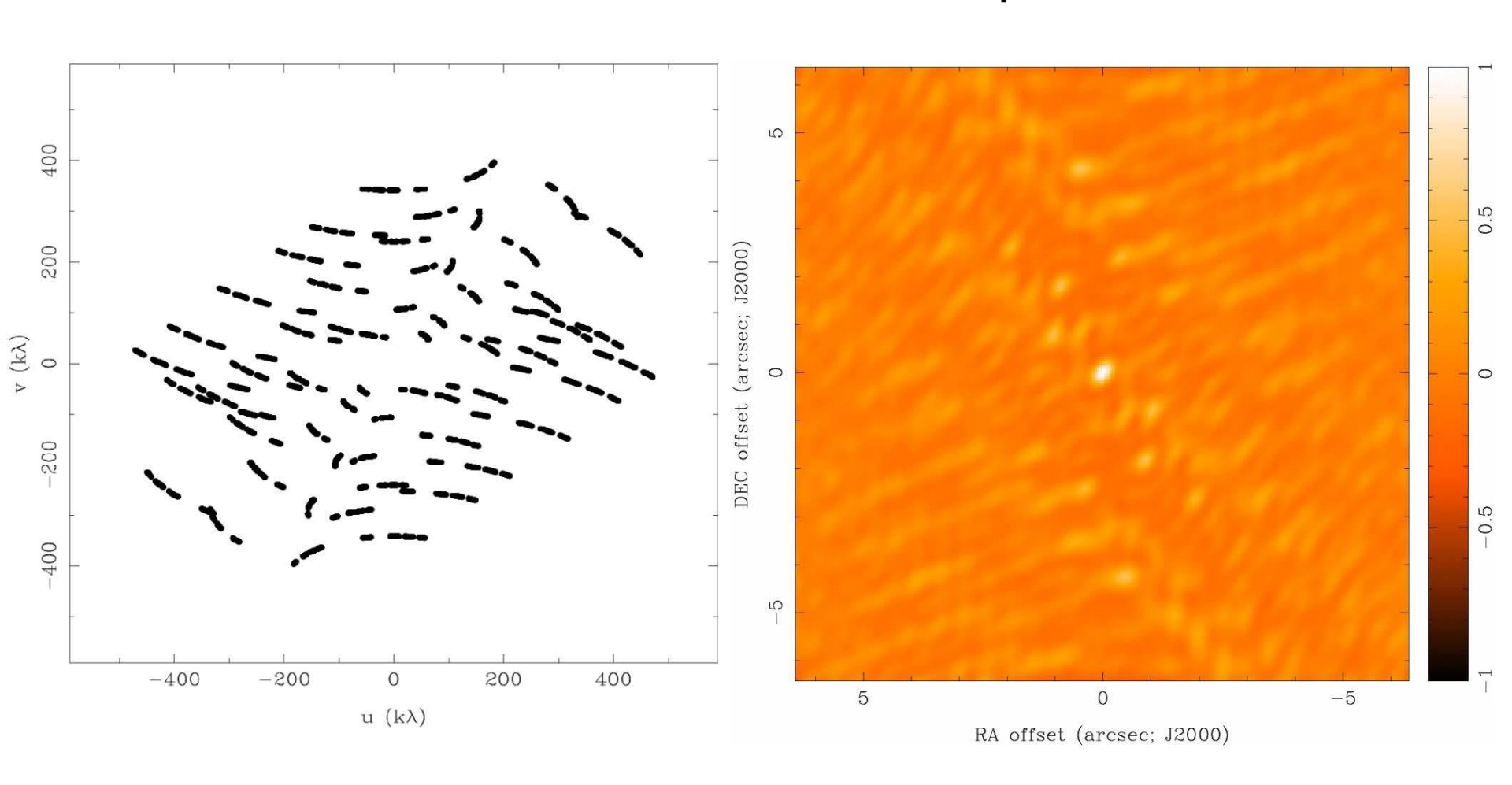
8 Antennas x 30 Samples



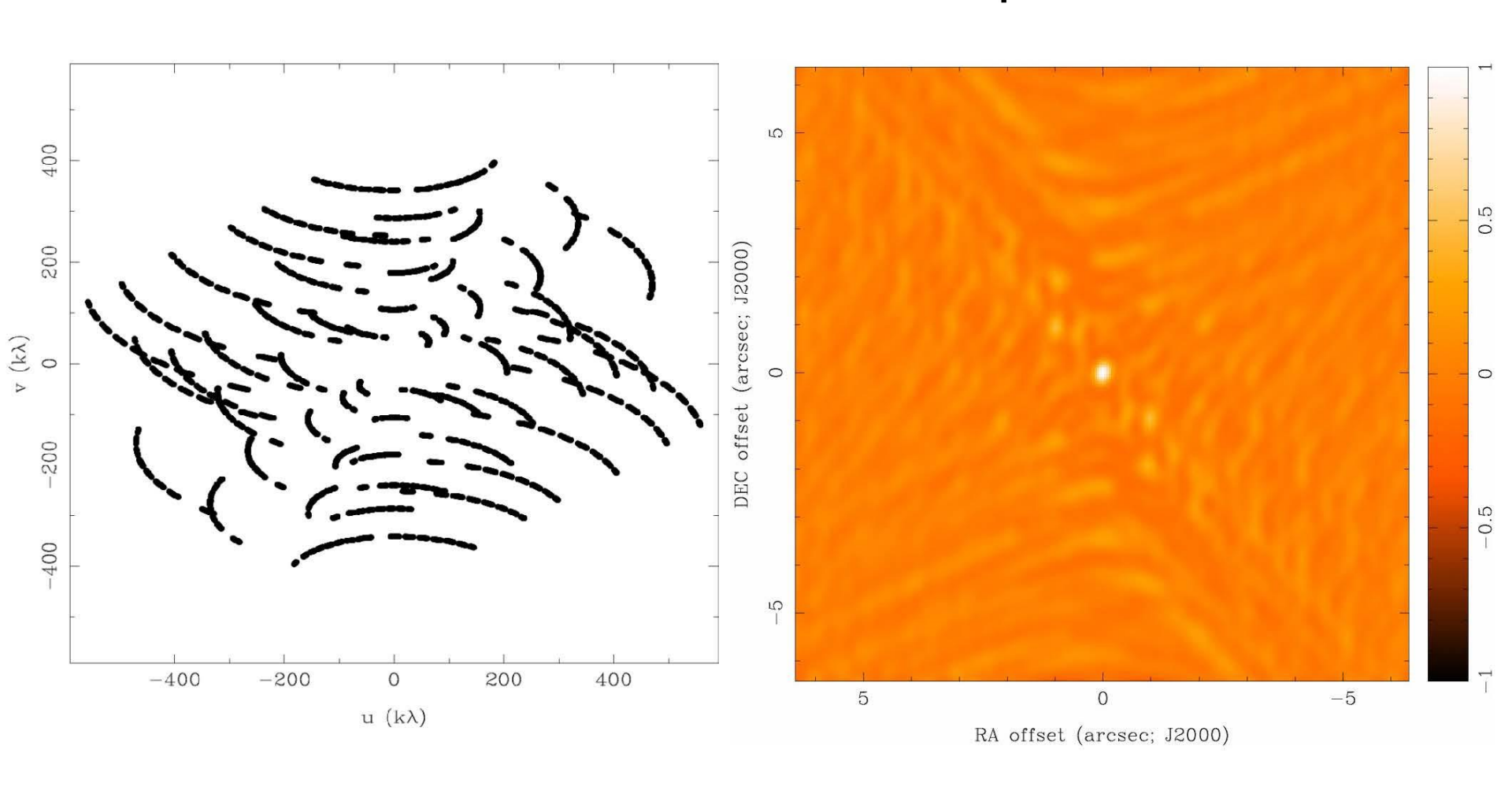
8 Antennas x 60 Samples



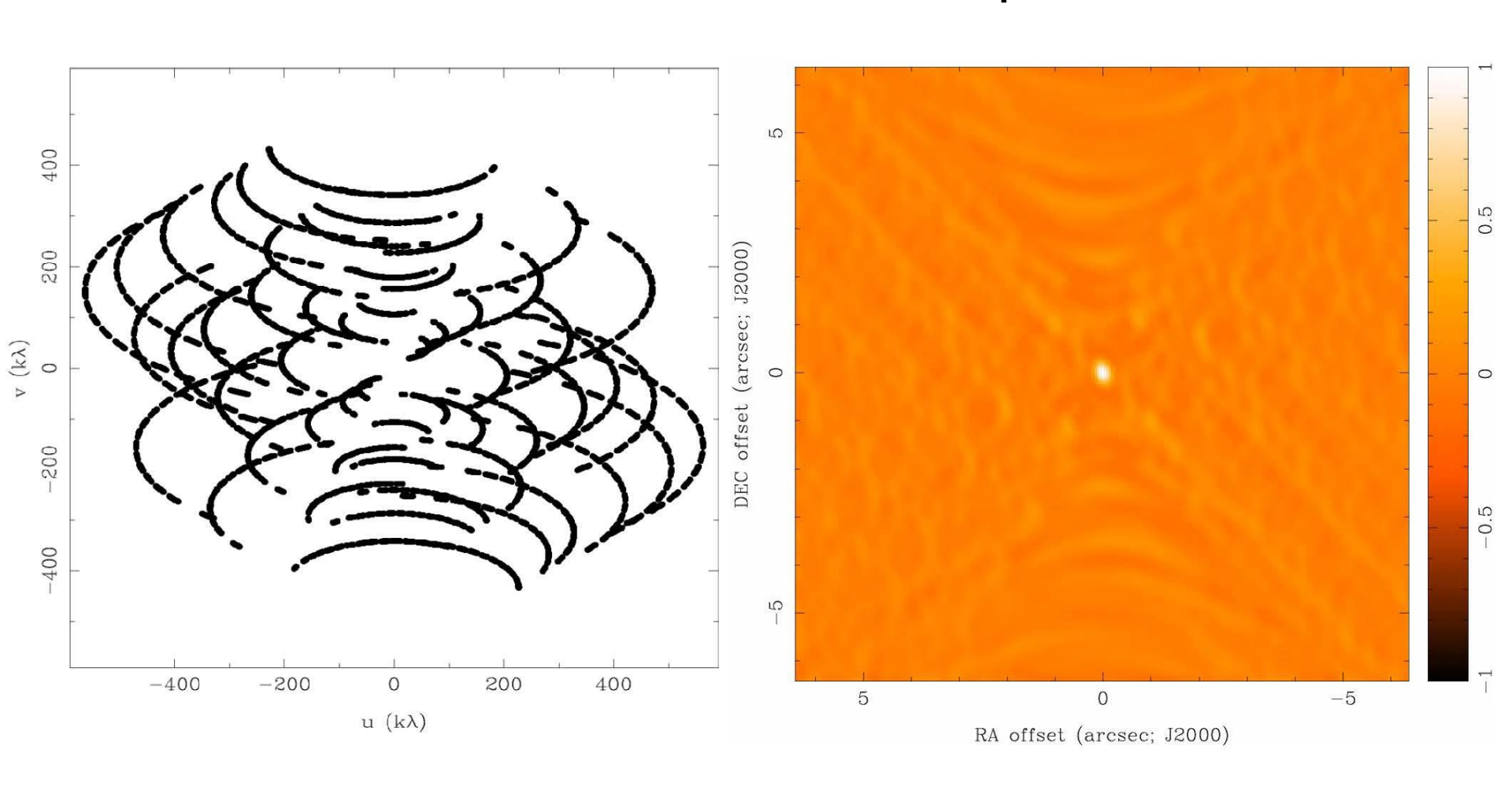
8 Antennas x 120 Samples



8 Antennas x 240 Samples

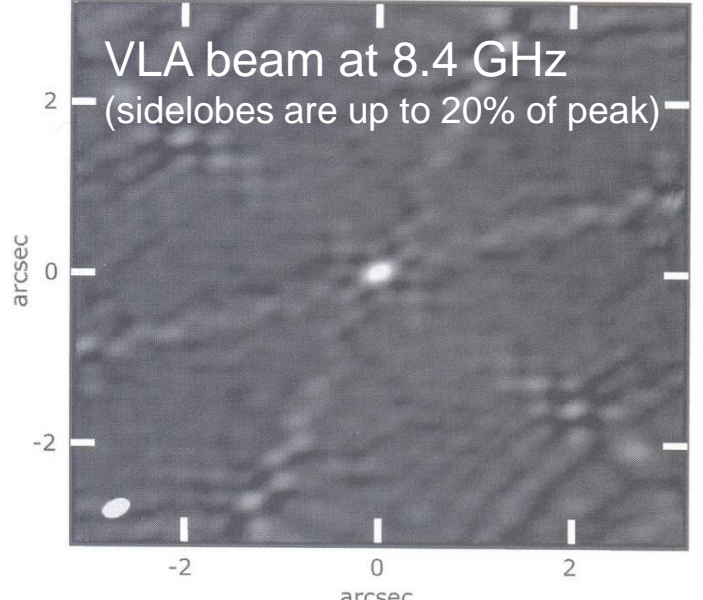


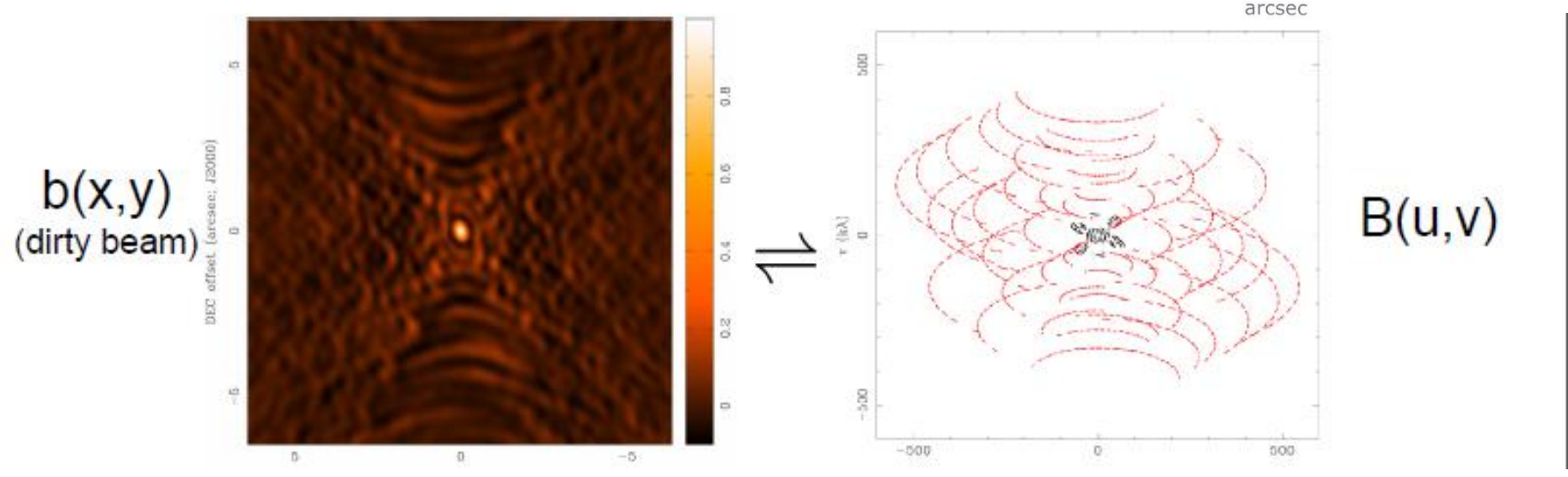
8 Antennas x 480 Samples



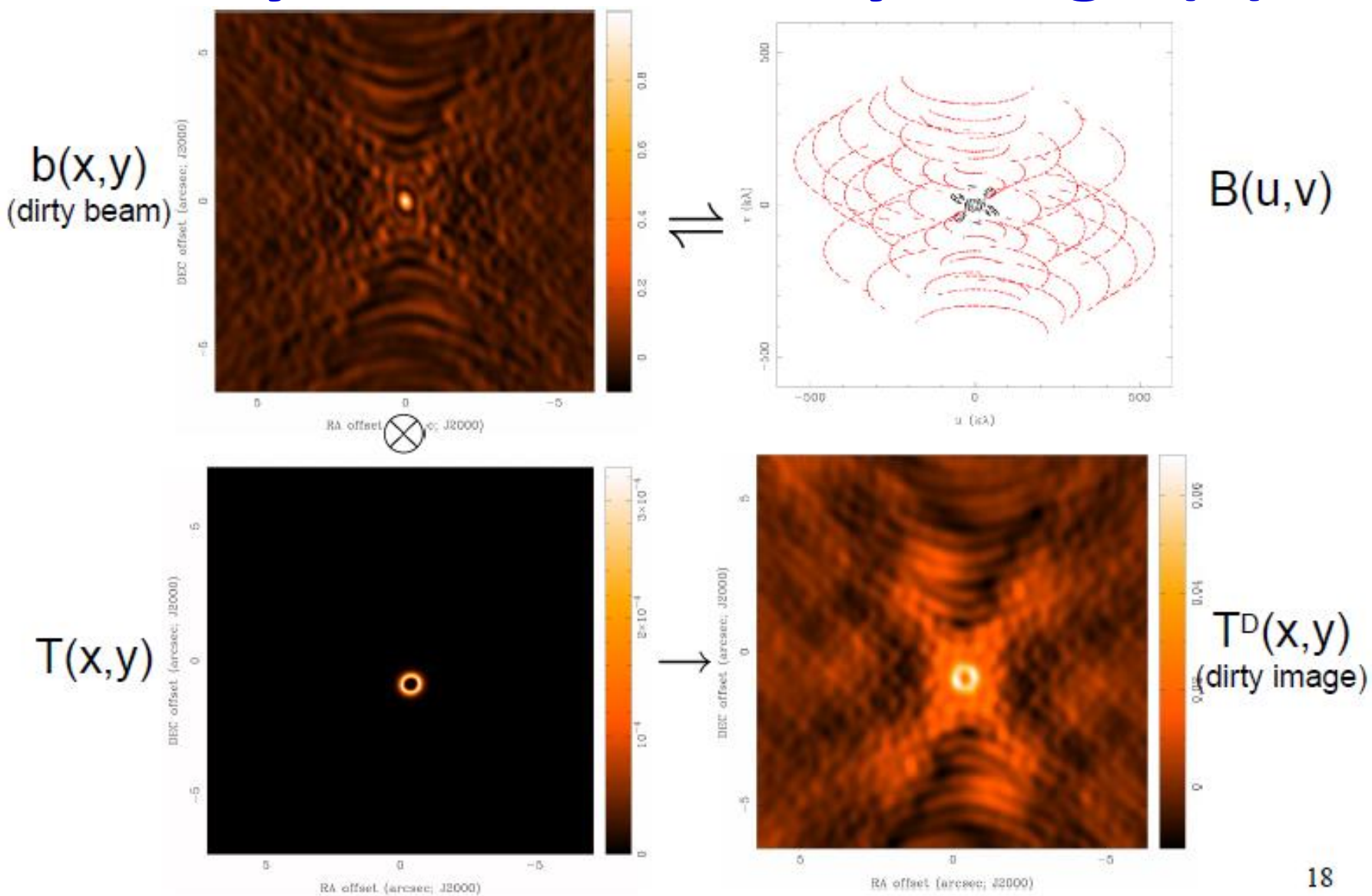
Dirty Beam and Dirty Image (1)

- interferometer array
 leave gaps in u,v-plane
- non-ideal PSF: dirty beam
- dirty beam makes dirty image



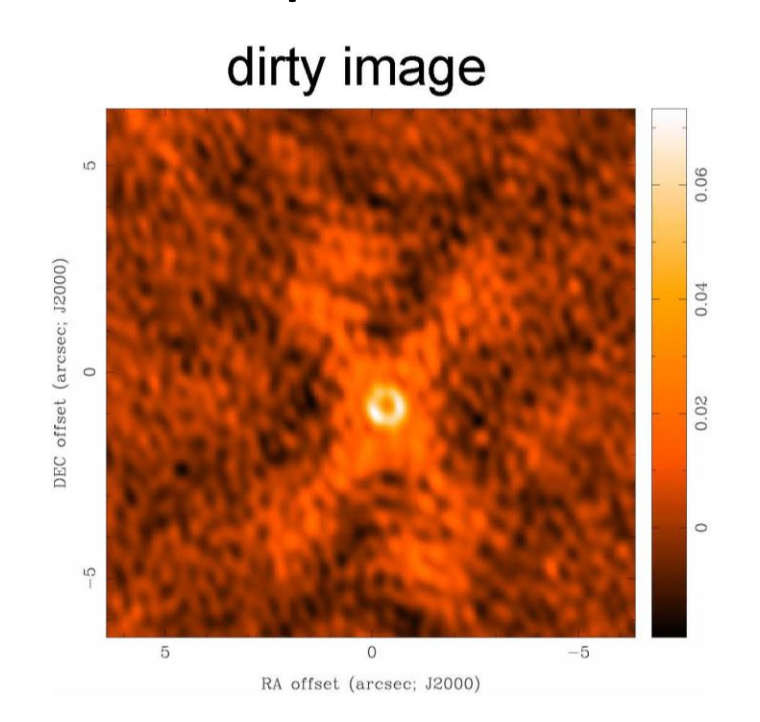


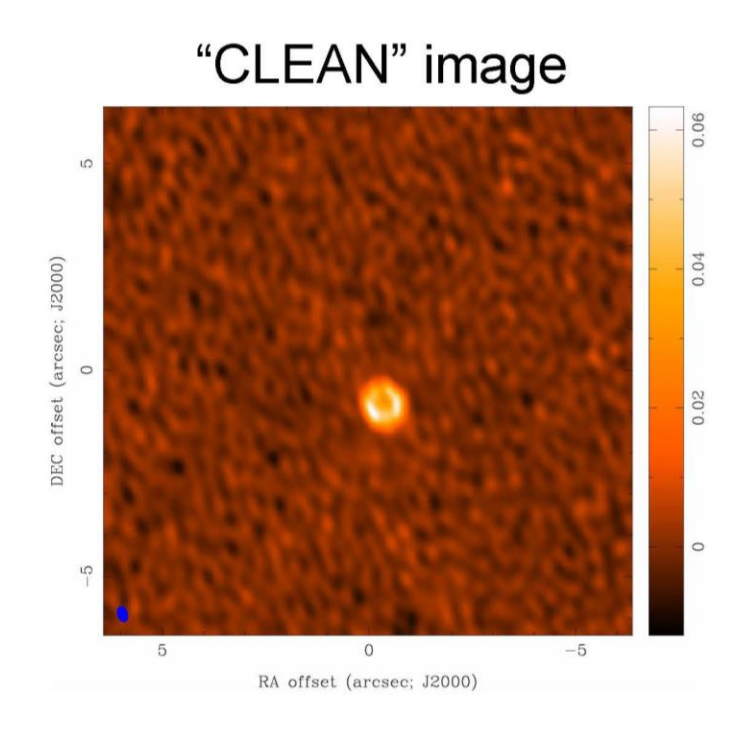
Dirty Beam and Dirty Image (2)



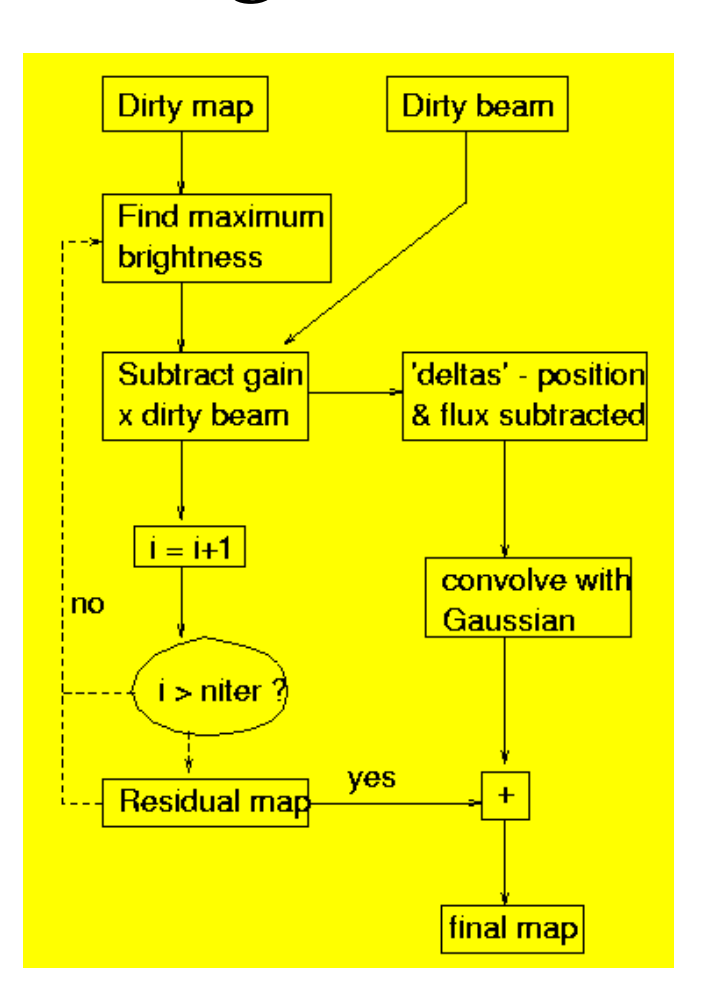
Deconvolution

- difficult to do science with dirty image
- deconvolve b(x,y) from $T^{D}(x,y)$ to recover T(x,y)
- information is missing and noise is present -> difficult problem





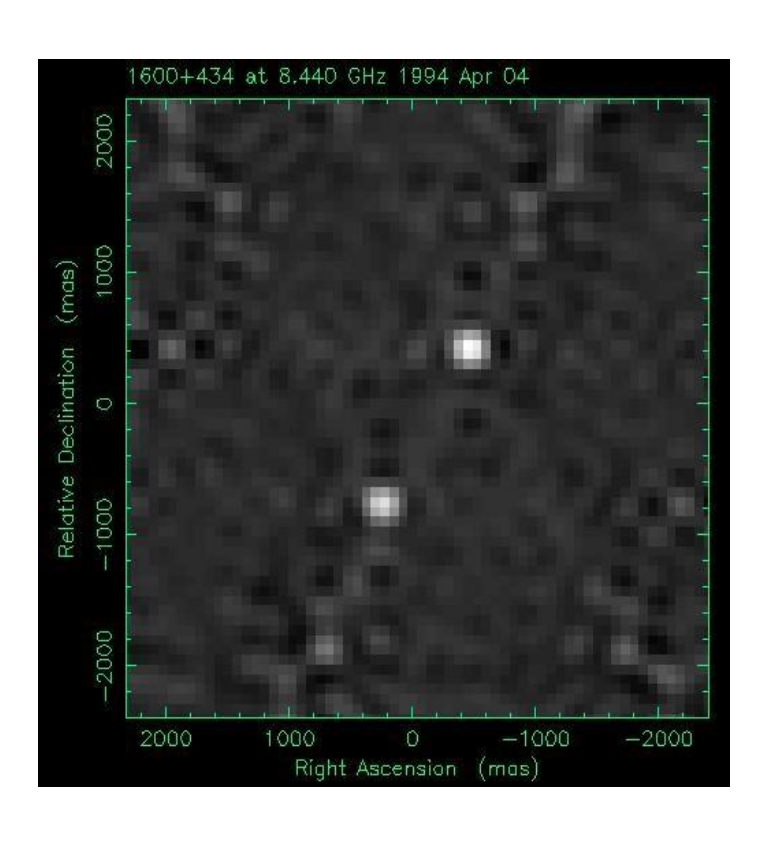
Hogbom CLEAN deconvolution

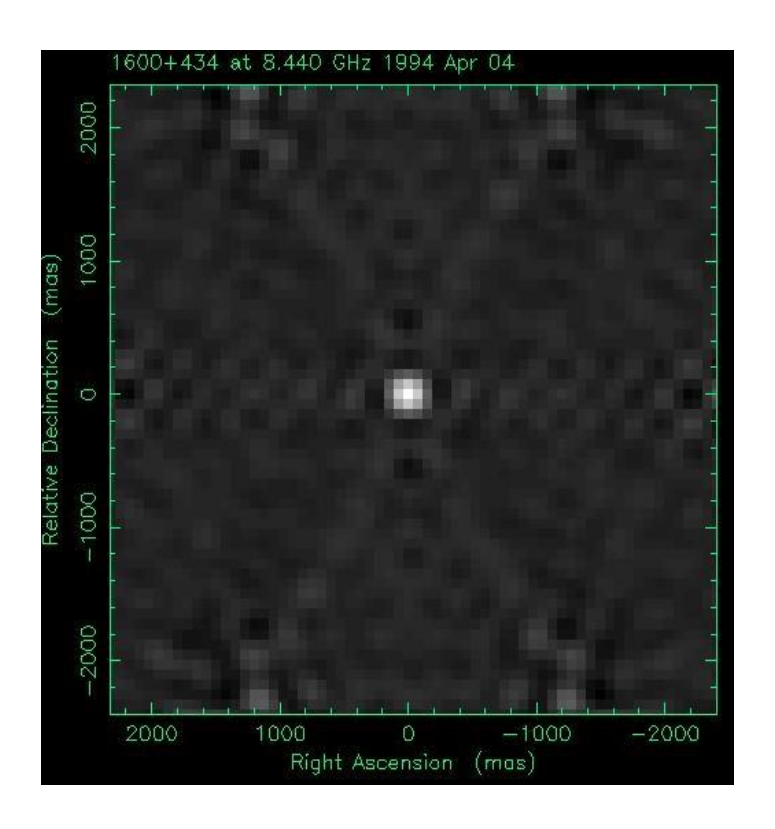


Brute-force iterative deconvolution using the dirty beam

Effectively reconstructs information in unsampled parts of the u-v plane by assuming sky is sum of point sources

(Quasi-) Hogbom CLEAN in action

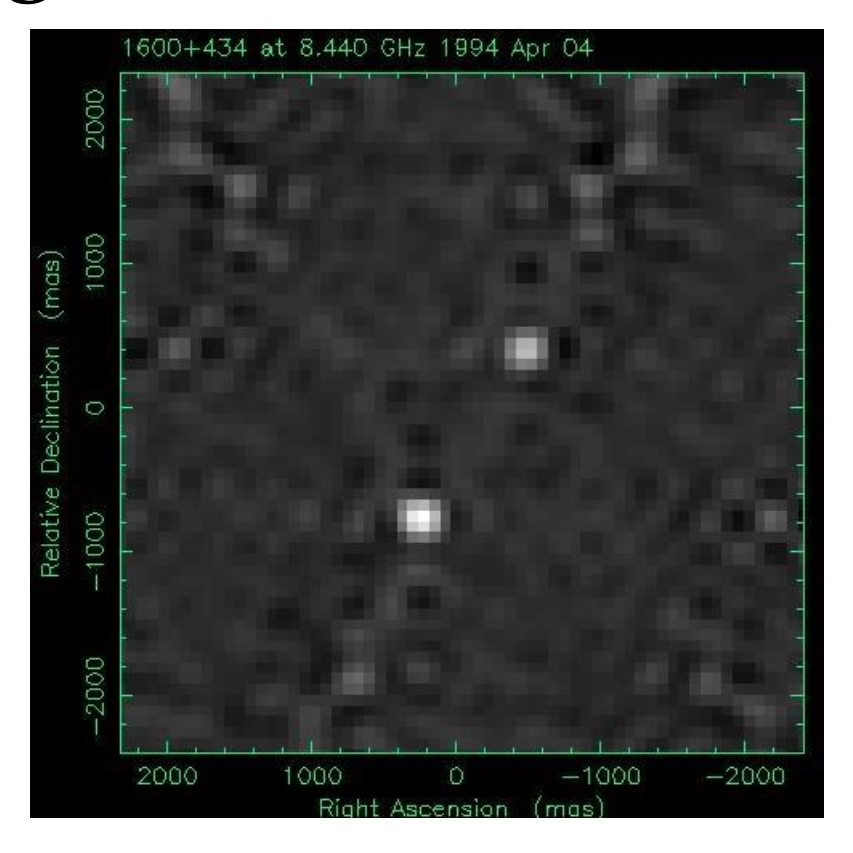




Dirty map

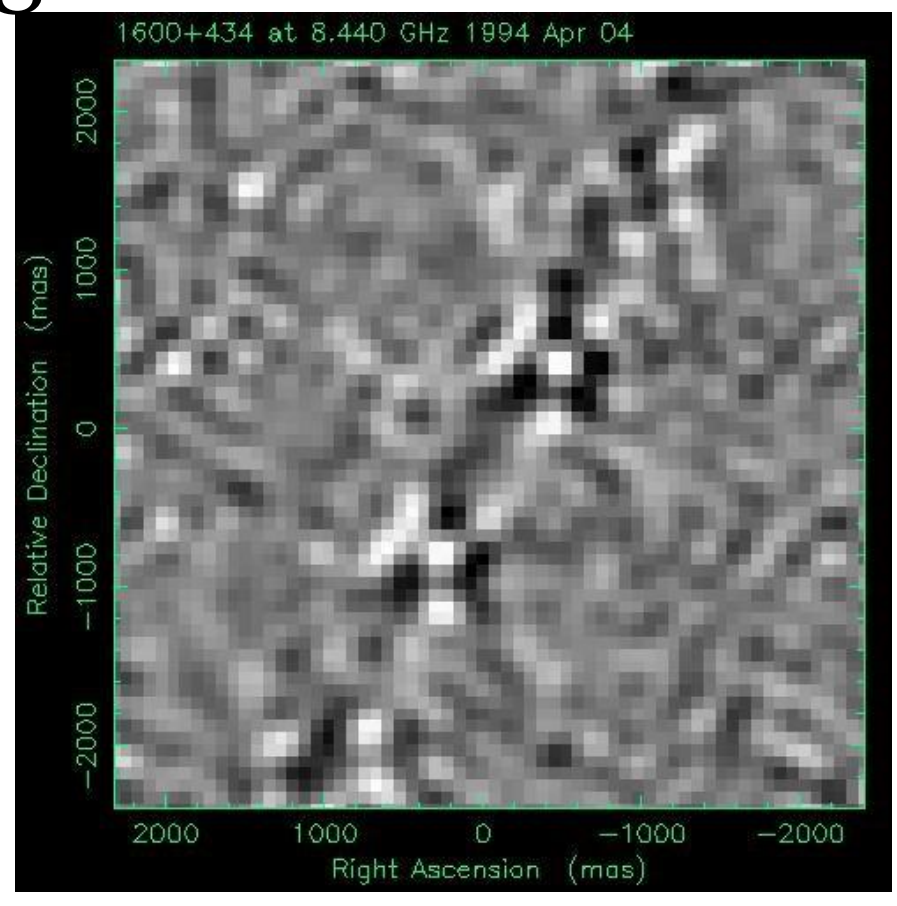
Dirty beam

Hogbom CLEAN in action



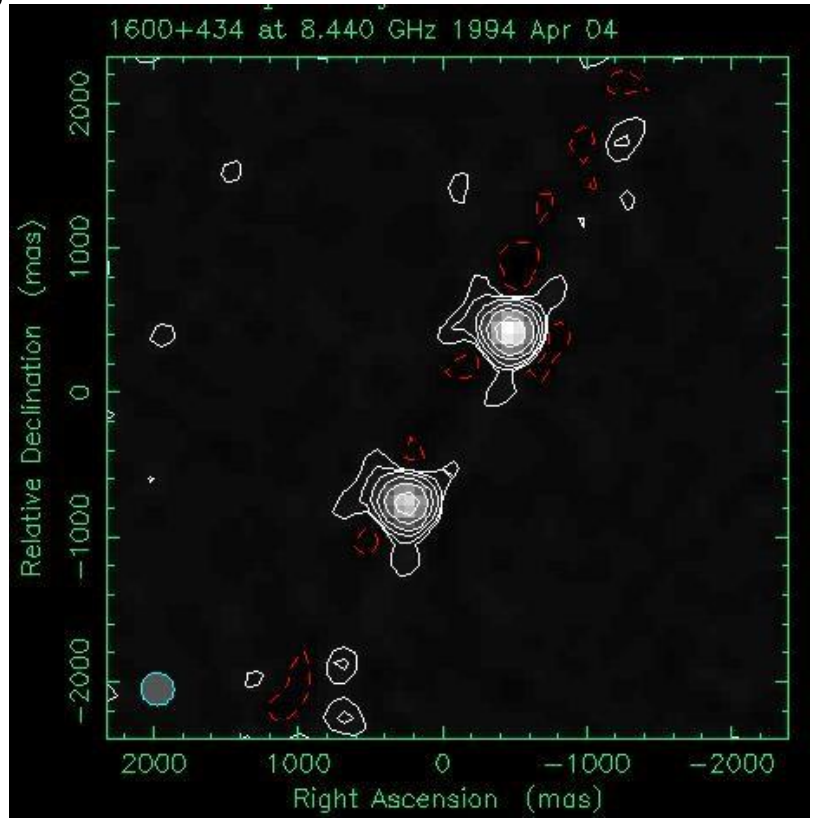
Residual after 1 CLEAN (gain 0.5)

Hogbom CLEAN in action



Residual after 100 CLEANs (gain 0.1)

Hogbom CLEAN in action



CLEAN map (residual+CCs) after 100 CLEANs (gain 0.1) Remaining artefacts due to phase corruption (see later lectures)

Self calibration

Calibrating a synthesis array is one of the most difficult aspects of its operation and, in many cases, is the most important factor in determining the quality of the final deconvolved image. Small quasi-random errors in the amplitude and phase calibration of the visibility data scatter power and so produce an increased level of "rumble" in the weaker regions of the image, and other systematic errors can lead to a variety of artifacts in the image.

The ordinary calibration procedure (see Lecture 5) relies on frequent observations of radio sources of known structure, strength and position in order to determine empirical corrections for time-variable instrumental and environmental factors that cannot be measured, or monitored, directly. The relationship between the visibility \tilde{V}_{ij} observed at time t on the i-j baseline and the true visibility $V_{ij}(t)$ can be written very generally as

$$\widetilde{V}_{ij}(t) = g_i(t)g_j^*(t)G_{ij}(t)V_{ij}(t) + \varepsilon_{ij}(t) \qquad (10-1)$$

The multiplicative factors $g_i(t)$ and $g_j(t)$ represent the effects of the complex gains of the array elements i and j; $G_{ij}(t)$ is the non-factorable part of the gain on the i-j baseline; $\varepsilon_{ij}(t)$ is an additive offset term; and $\epsilon_{ij}(t)$ is a pure, zeromean, noise term representing the thermal noise. The effects of $G_{ij}(t)$ and $\varepsilon_{ij}(t)$, which cannot be split into antenna-dependent parts, can usually be reduced to a satisfactory degree by clever design (see Lecture 4), so we will ignore them during this lecture. Equation 10–1 then simplifies to

$$\tilde{V}_{ij}(t) = g_i(t)g_j^*(t)V_{ij}(t) + \epsilon_{ij}(t)$$
. (10–2)

The element gain (usually called the antenna gain in radio astronomy) really describes the properties of the elements relative to some reference (usually one array element for phase and a "mean" array element for amplitude). Although this use of the word "gain" may seem confusing, it is quite helpful in lumping all element-based properties together. The gain for any one array element has two contributing components: firstly, a slowly varying instrumental part and secondly, a more rapidly varying part due to the atmosphere (troposphere and ionosphere) above the element. Variations in the phase part of the atmospheric component nearly always dominate the overall variation of the element gains (see Sec. 4 of Lecture 5).

Selfcalibration

- 1. Start with a decent image of the sky
- 2. Calculate $V_{ij}(t)$ from a Fourier transform of this sky image
- 3. Solve eq. 10-2 for gains $g_i(t)$
 - note that this can been done since N telescopes (with N gains $g_i(t)$) give N(N-1)/2 ~ N² visibilities
- 4. Produce improved image using better calibrated visibilities
- 5. Repeat 2-4 with improved image, until no further improvement

Interferometer Components

Optical Interferometer

- Telescopes
- Delay Lines
- Beam Combiner
- Fringe Tracker
- Detector

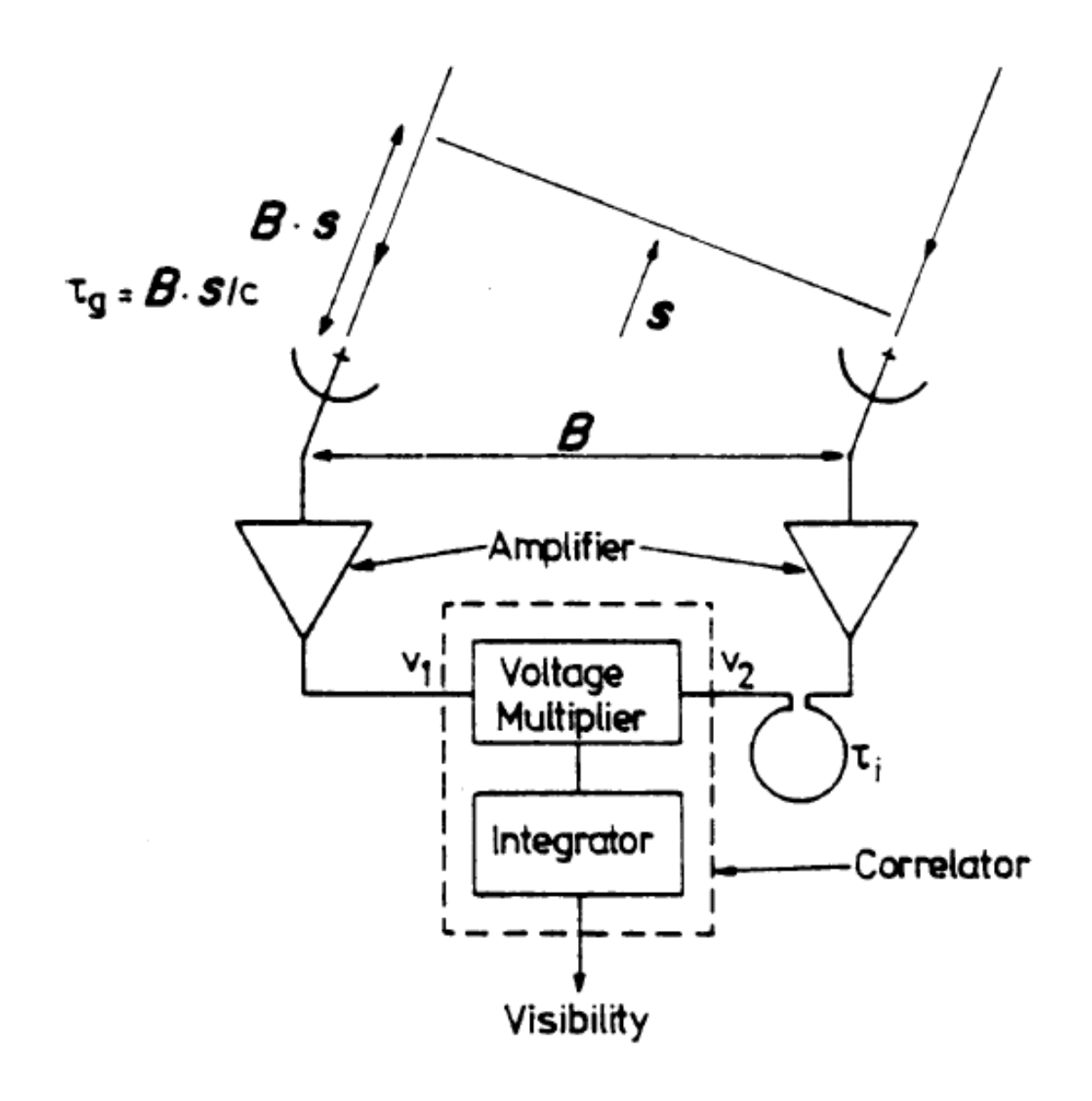
Measures amplitude of visibilities

Radio Interferometer

- Telescopes
- Receiver
- Signal Delay
- Correlator

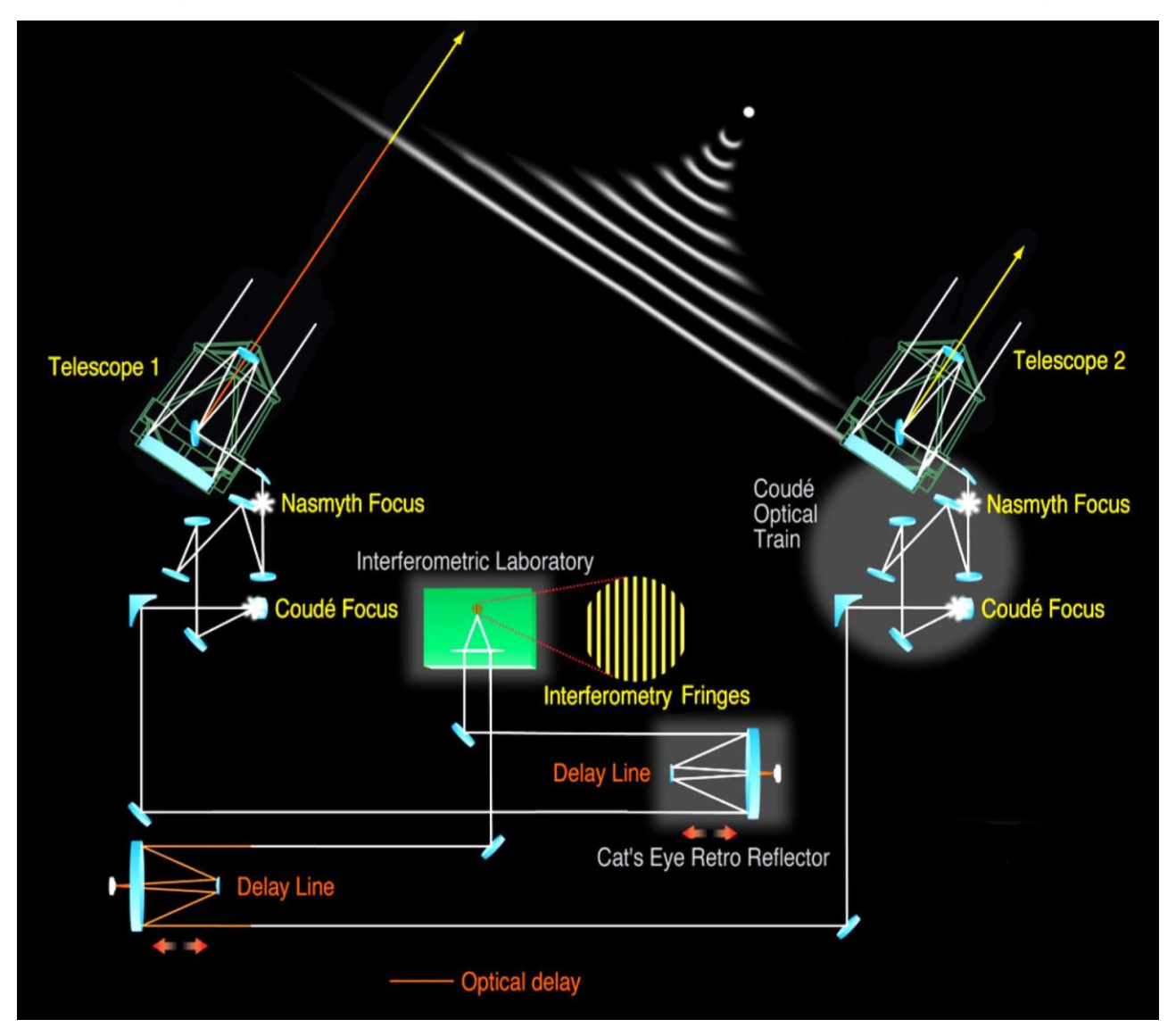
Measures complex visibilities

Radio Interferometry



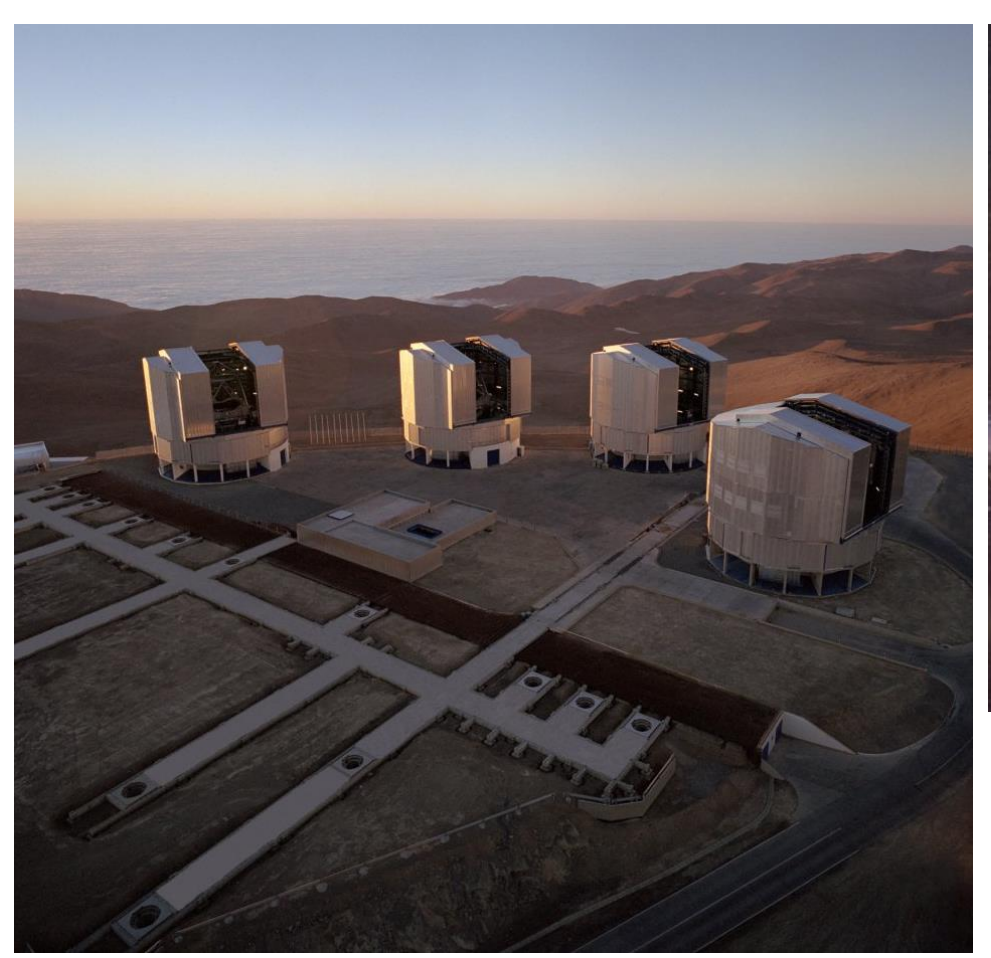
- Radio heterodyne receiver output retains phase information of incoming signal
- Adjustable signal delay
- Correlator: average product of two signals

Optical Interferometry



Telescopes

Optical interferometer consists of $n \ge 2$ telescopes of similar type



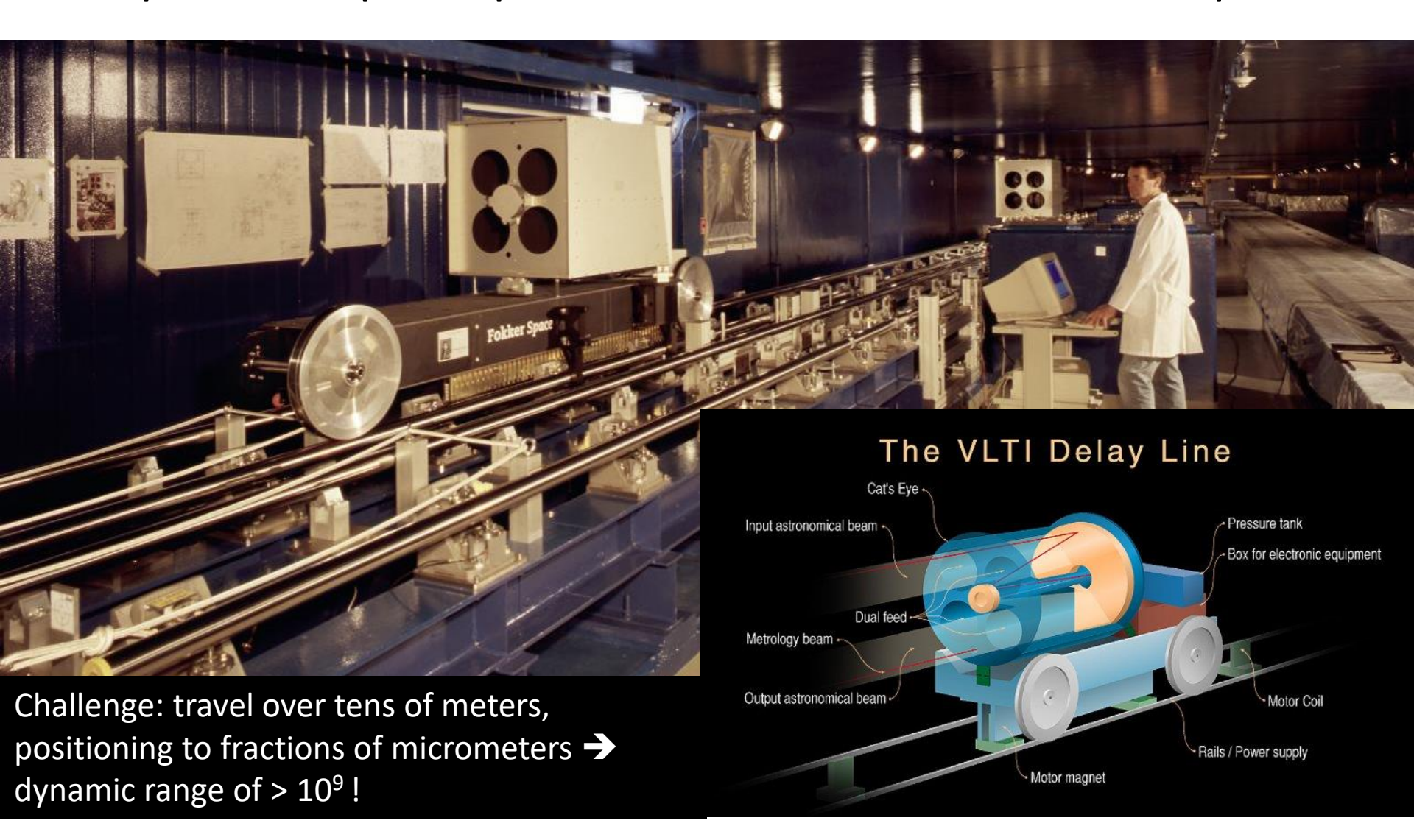


Keck interferometer (Hawaii) 🛧

← VLTI (Paranal)

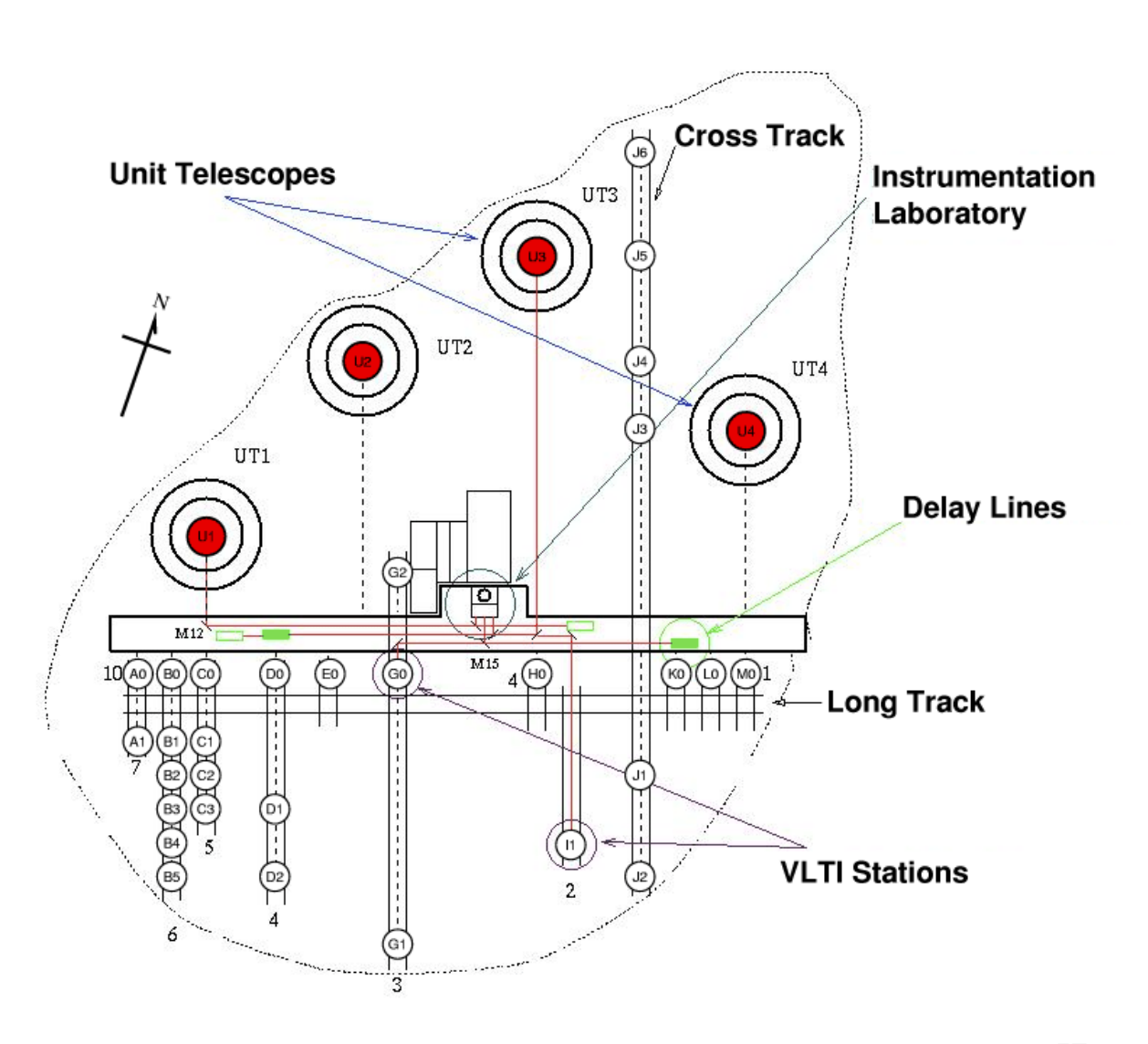
Delay Lines

Compensate optical path difference between telescopes



Optical: VLTI Baselines

3 ATs move on rails between 30 observing stations above the holes that provide access to the underlying tunnel system. The light beams from the individual telescopes are guided towards the centrally located, partly underground Interferometry Laboratory



Australia Telescope Compact Array ATCA

Six 22 m telescopes on an east-west baseline



Westerbork

- Westerbork
 Synthesis Radio
 Telescope
 (WSRT)
- 14 telescopes
- 25-m diameter
- East-west baseline
- 3 km in length
- effective collecting area of a 92 m dish



LOFAR in the Netherlands

LOw Frequency ARray uses two types of low-cost antennas:

- Low Band Antenna (10-90 MHz) -
- High Band Antenna (110-250 MHz)

Antennae are organized in 36 stations over ~100 km. Each station contains 96 LBAs and 48 HBAs

Baselines: 100m - 1500km

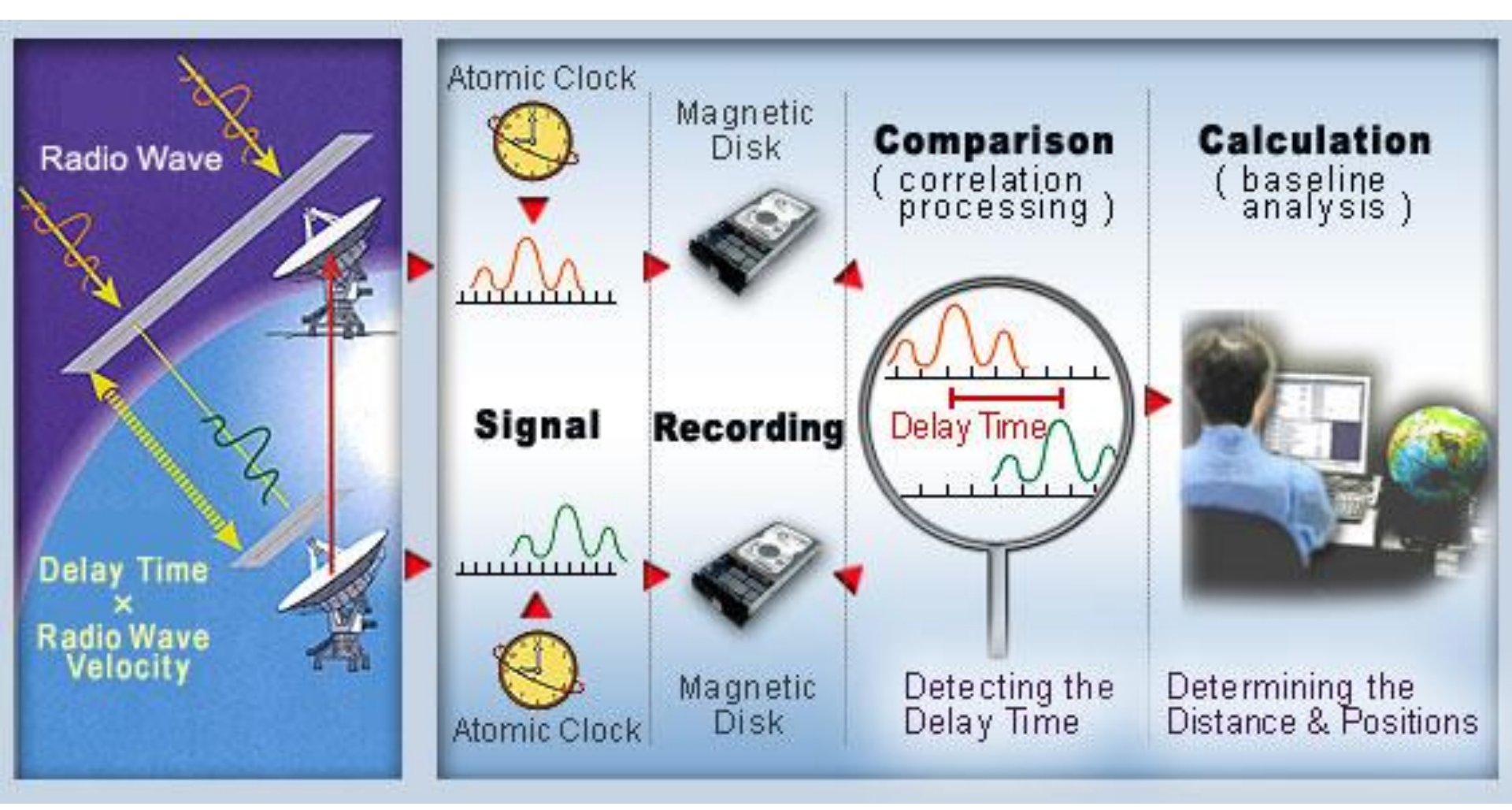








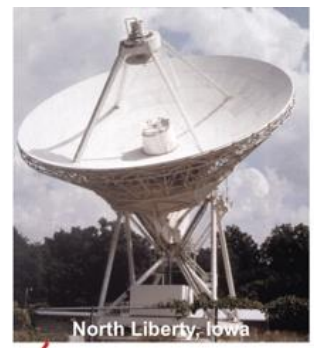
The Very Long Baseline Interferometer (VLBI) Technique



Very Long Baseline Array VLBA (USA)









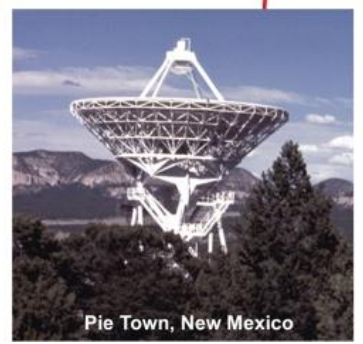
Ten 25 m antennas form an array of 8000 km in size.

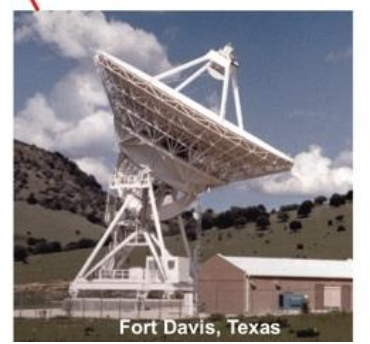


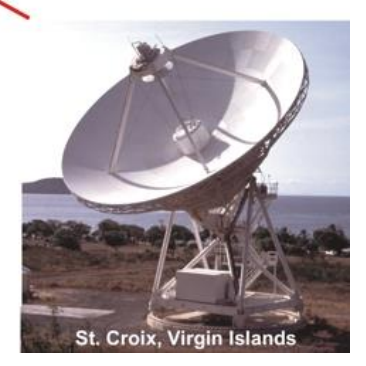






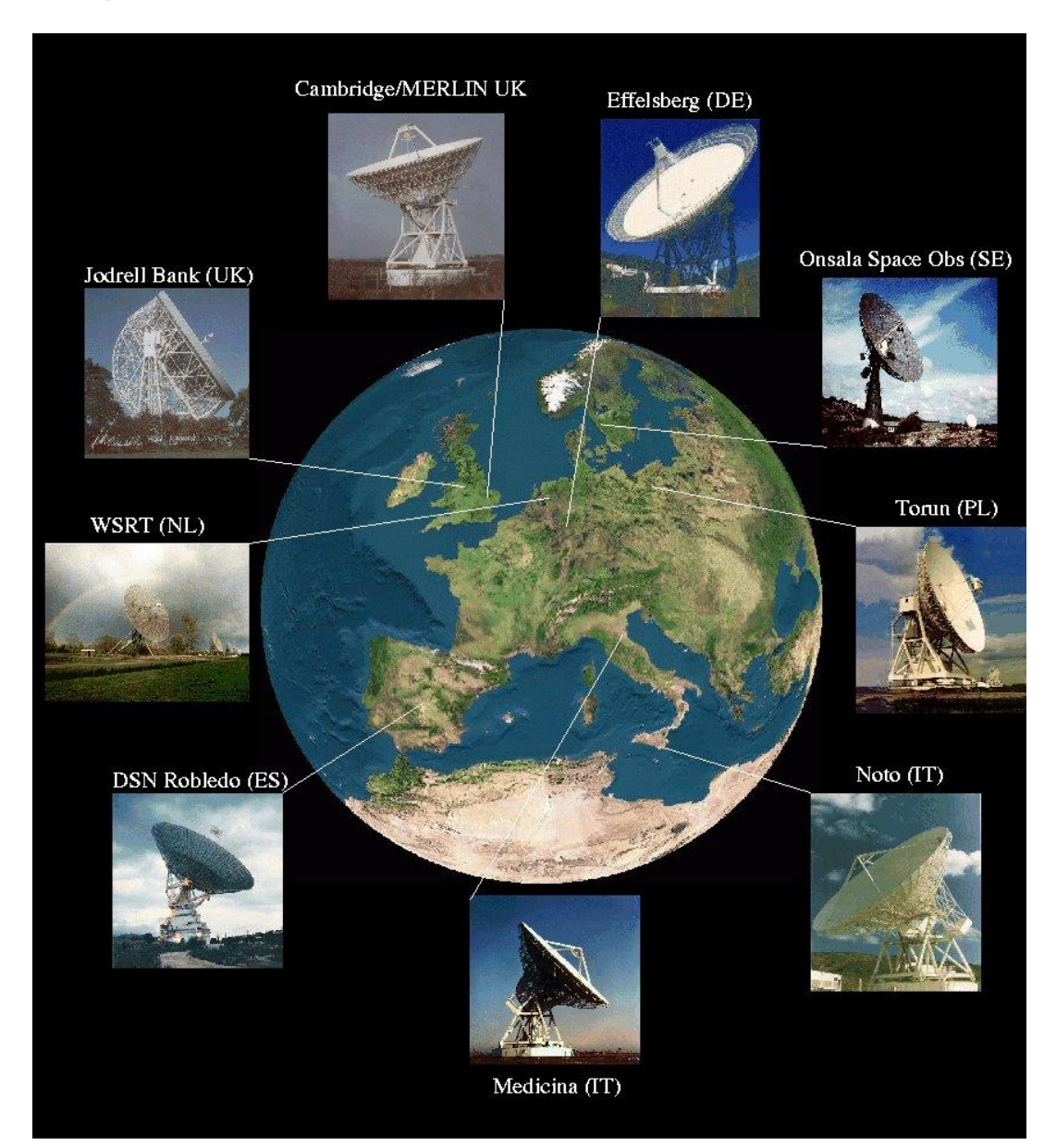


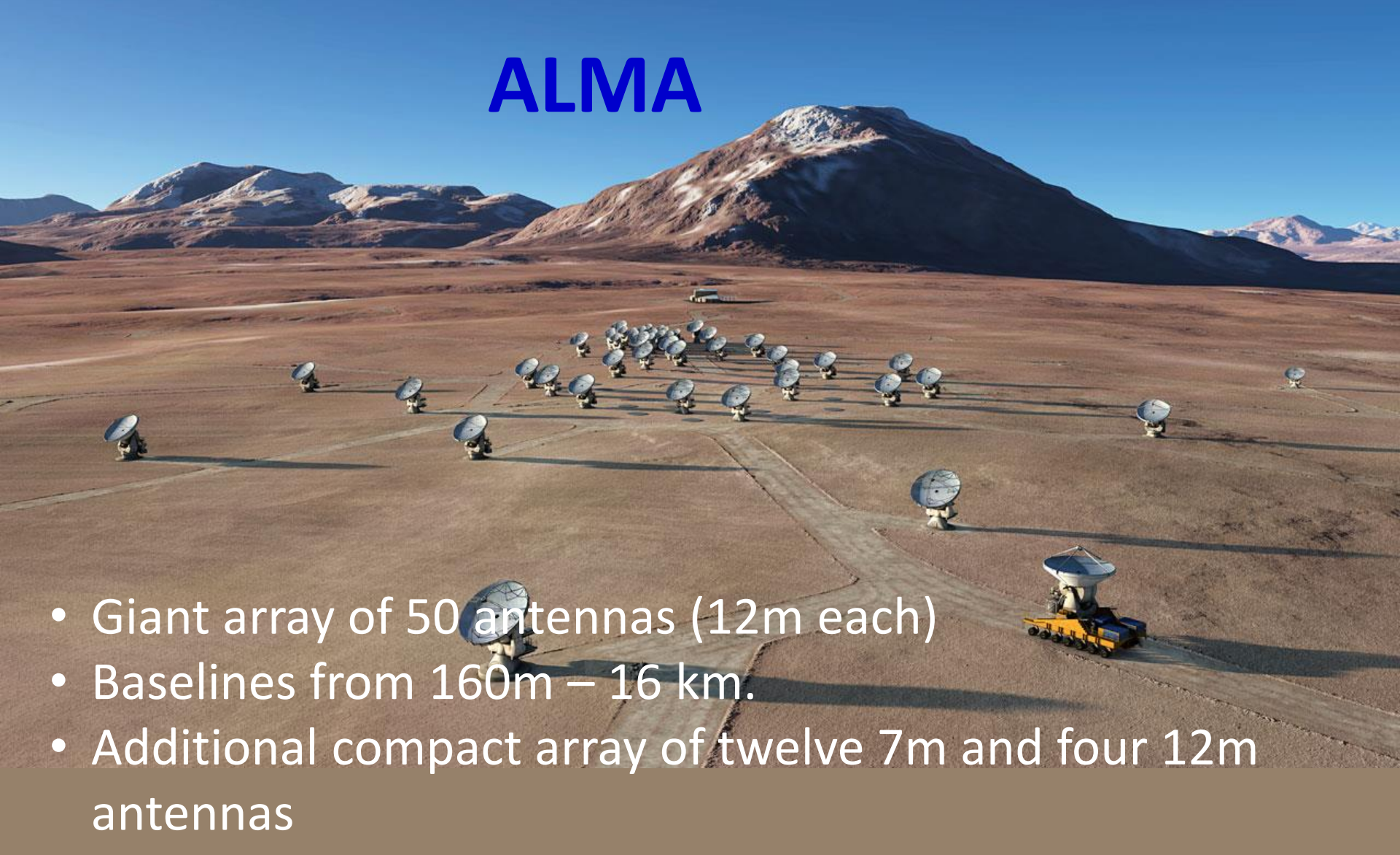




VLBI in Europe: European VLBI Network (EVN)

- now possible to connect VLBI radio telescopes in real-time
 → e-VLBI
- In Europe, six radio telescopes of the EVN are now connected with Gbit/s-links
- Data processing in real time at the European Data Processing centre at JIVE (Astron/Dwingeloo)





- Located on the Chajnantor plain at 5000m altitude
- Wavelength range 3 mm 400 μm (84 to 720 GHz)

ALMA

- Frequencies: Band 3 (>84 GHz) to band 9 (<720 GHz).
- Field of view depends on antenna diameter and frequency
 - independent of array configuration!
 - FWHM of beam: 21" at 300 GHz
 - uniform sensitivity over larger field requires mosaicking
- Spatial resolution depends on frequency & maximum baseline
 - Most extended configuration (~16 km): 6 mas at 675 GHz
 - Structures > 0.6»λ/b_{min} (b_{min}=shortest baseline) are not well reproduced in reconstructed images → measure with the ALMA Compact Array (ACA) using the 7-m antennae (come closer)
- Spectral resolution: up to 8192 frequency channels (spectral resolution elements). At 110 GHz, R=30,000,000 or 10m/s velocity resolution.





HL Tau



References

Synthesis imaging. Course notes from an NRAO summer school, held at Socorro, New Mexico, USA, 5 - 9 August 1985.. R. A. Perley, F. R. Schwab, A. H. Bridle (Editors)

http://www.phys.unm.edu/~gbtaylor/astr423/s98book.pdf

 https://www.astro.rug.nl/~mcctskads/lecture_deBruyn.pdf